Nuclear structure of ^{112}Cd studied through the ^{111}Cd($\vec{d}$, p) reaction

D. S. Jamieson,[1,*] P. E. Garrett,[1,2,†] G. C. Ball,[3] G. A. Demand,[1] T. Faestermann,[4] P. Finlay,[1] K. L. Green,[1] R. Hertenberger,[5] K. G. Leach,[1,‡] A. A. Phillips,[1] C. S. Sumithrarachchi,[1,§] S. Triambak,[2,6] and H.-F. Wirth[5]

[1]*Department of Physics, University of Guelph, Guelph, Ontario N1G2W1, Canada*
[2]*Department of Physics and Astronomy, University of the Western Cape, P/B X17, Bellville ZA-7535, South Africa*
[3]*TRIUMF, 4004 Wesbrook Mall, Vancouver, British Columbia V6T 2A3, Canada*
[4]*Physik Department, Technische Universität München, D-85748 Garching, Germany*
[5]*Fakulat für Physik, Ludwig-Maximilians-Universität München, D-85748 Garching, Germany*
[6]*iThemba LABS, National Research Foundation, P.O. Box 722, 7129 Somerset West, South Africa*

(Received 7 June 2018; revised manuscript received 26 August 2018; published 10 October 2018)

The nuclear structure of ^{112}Cd has been investigated with the ^{111}Cd($\vec{d}$, p)^{112}Cd reaction. Isotopically enriched targets of ^{111}Cd were bombarded with 22 MeV polarized deuterons, and reaction products were analyzed with a magnetic spectrograph. Angular distributions and analyzing powers were determined for 129 states, 49 of which are newly observed, up to approximately 4.2 MeV in excitation energy. The observed angular distributions were compared with distorted wave Born approximation (DWBA) and adiabatic distorted wave approximation (ADWA) calculations to extract the spectroscopic factors. Two-quasineutron configurations involving coupling to the $s_{\frac{1}{2}}$ orbital are suggested. The sum of spectroscopic strengths extracted by using the ADWA for the individual l transfers are combined with previous results from the ^{111}Cd($\vec{d}$, t) reaction and show good agreement with the $2j+1$ sum rule, whereas those extracted with the DWBA calculations are significantly less.

DOI: 10.1103/PhysRevC.98.044309

I. MOTIVATION

The cadmium isotopes, especially ^{110,112}Cd, have been pivotal nuclei for the development of nuclear structure models and have often been cited as paradigms for harmonic spherical vibrational motion [1]. Indeed, the appearance of a nearly degenerate set of states with spin-parities 0^+, 2^+, and 4^+ at twice the energy of the first 2^+ state, together with enhanced $E2$ transition rates to the $2_1{}^+$ state, have been used to classify the mid-shell Cd isotopes as excellent examples of nuclei manifesting the U(5) limit of the interacting boson model (IBM) [1]. Recent studies [2–6], however, have cast doubt on the appropriateness of this description.

The mid-shell Cd isotopes have been extensively examined by using γ-ray spectroscopy. Studies made with compound nucleus fusion evaporation reactions (see, e.g., Refs. [7–15]) provided detailed level schemes over a wide spin range, and elucidated the systematics of the shape-coexisting intruder bands. Additional details on low-spin states, and level lifetimes, were provided by measurements with the $(n, n'\gamma)$ reaction [4,16–21], and recently β-decay studies have revealed weak, low-energy γ-ray decay branches between highly excited states [4,14,15,22–26]. However, the Cd isotopes have not been as extensively examined with transfer reactions. A very detailed set of Cd($\vec{d}$, t) measurements with 20 and 22 MeV polarized deuteron beams was made some 20–25 years ago [27,28], and the previous (d, p) reactions to study ^{112,114}Cd were performed 50 years ago [29,30] using 7.7 and 7.5 MeV deuteron beams, respectively. The low beam energies used in the (d, p) reactions limited the amount of angular momentum in the system; a consequence of this is that states with high-l transfers were weakly populated and easily overlooked. Because the previous (d, p) measurements were rather limited by the beam energy used, and given the increase in the knowledge of the ^{112}Cd level scheme, it was deemed useful to repeat the ^{111}Cd(d, p) measurement at a much higher beam energy, as well as employing the powerful Q3D spectrograph (Maier-Leibnitz Laboratory, Garching) to achieve a high resolution. In addition, the availability of a polarized deuteron ion source provided the opportunity to measure analyzing powers, increasing the amount of information that could be obtained on the nature of the transfer.

Single-nucleon transfer reactions provide information on the single-particle content of the wave functions [31]. Starting with an odd-A target where the ground state wave function can be described as a one-quasiparticle configuration, the (d, p) stripping reaction populates two quasiparticle states, and preferentially those above the Fermi surface. In the case of the ^{111}Cd(d, p) reaction, the target ground state wave function is $\nu s_{\frac{1}{2}}$, and thus final states of the form $\nu s_{\frac{1}{2}} \otimes j_{\rm tr}$ are populated, where $j_{\rm tr}$ is the configuration of the transfer particle.

*Present address: Department of Physics, Stony Brook University, Stony Brook, NY, USA; andrew.jamieson@stonybrook.edu
†pgarrett@physics.uoguelph.ca
‡Present address: Department of Physics, Colorado School of Mines, Golden, CO 80401, USA.
§Present address: National Superconducting Cyclotron Center, Michigan State University, East Lansing, MI 48824, USA.

 ©2018 American Physical Society

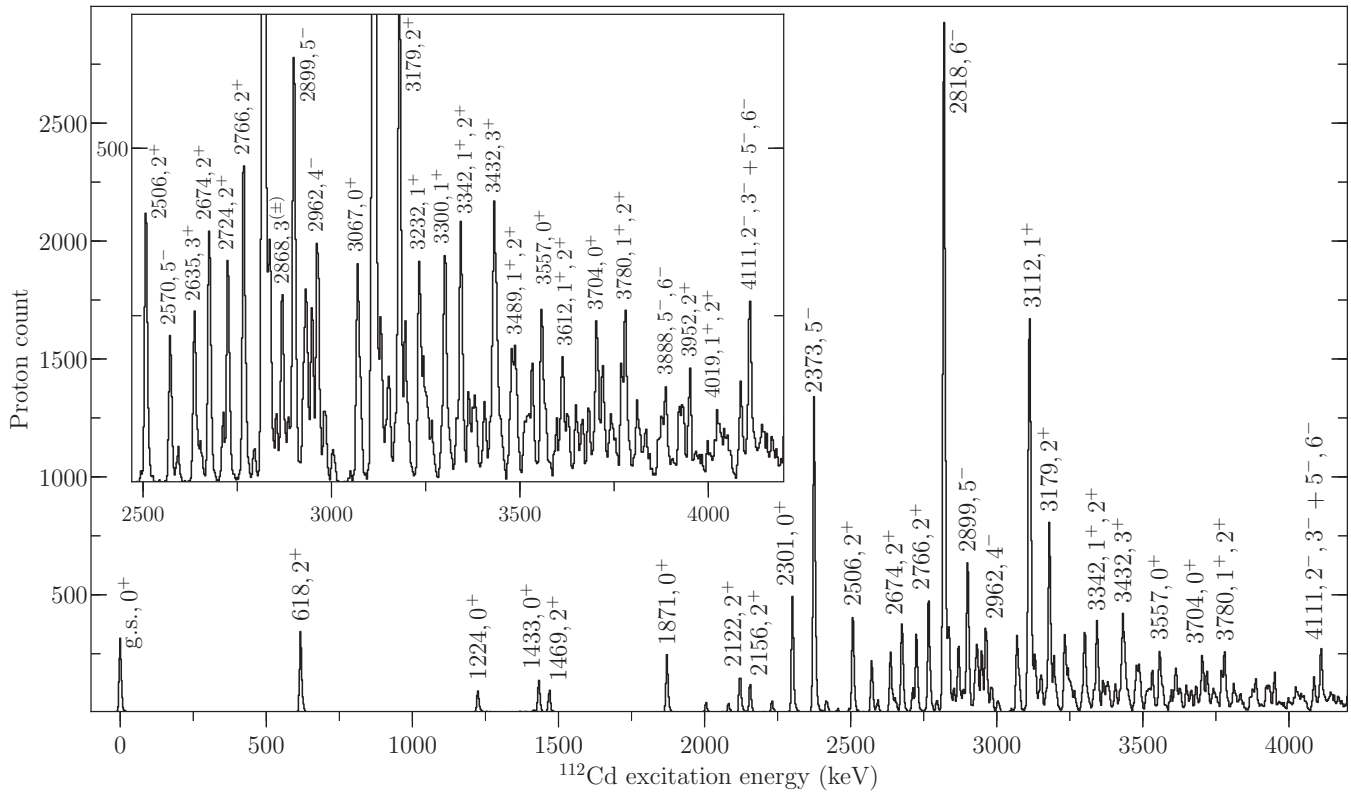

FIG. 1. Proton spectrum observed following the ^{111}Cd($\vec{d}$, p) reaction with 22 MeV deuteron beams. The spectrum was collected with two momentum settings for the magnets and the high-momentum and low-momentum spectra have been combined and normalized. The spectra were energy calibrated with a cubic polynomial. The inset shows the spectrum in detail above 2400 keV.

Since investigations of the collective states in the Cd nuclei, especially ^{110,112}Cd, has been extending into regions above the pairing gap, it is important to have knowledge of the single-particle content of the wave functions to check the consistency of the assignments; states populated strongly in a single-nucleon transfer reaction must be two-quasiparticle states or one-phonon states (which are composed of two-quasiparticle configurations). This argument was used recently [32], based on data obtained as part of the present work, to overturn an earlier assignment [33] of the 5^- member of the quadrupole-octupole coupled state in ^{112}Cd. In the present work, the full results of the ^{111}Cd($\vec{d}$, p) measurement are reported.

II. EXPERIMENT

The high-resolution single-neutron-transfer reaction experiment was performed at the Maier-Leibnitz Laboratory [34] in Garching, Germany. A polarized beam of deuterons was accelerated to an energy of 22 MeV by using the 14 MV tandem Van de Graaff accelerator, with 80(4)% polarization achieved [35]. The deuteron beam impinged on a 159 ± 6 μg cm^{-2} target enriched to >99% in ^{111}Cd. The outgoing protons from the reaction were momentum analyzed with the Q3D magnetic spectrograph, and detected with a position-sensitive cathode-strip detector for particle identification [36]. Proton spectra resulting from the transfer reaction were collected over two different magnetic field settings of the Q3D for each angle. The lower excitation energy range (the high-momentum bite) covered the range from the ground state of ^{112}Cd to approximately 2.4 MeV in excitation energy. The higher excitation energy range (the low-momentum bite) used a magnet setting appropriate for the energy range from 2.0 to 4.2 MeV. The transfer data were collected at angles from 10° to 50° in 5° increments for both magnetic field settings, with additional data at an angle of 60° taken for the low-momentum bite. Two spectra were taken at each angle and magnetic field setting, one for each beam polarization. Figure 1 shows an example of a spectrum obtained during the experiment, and shows both the high quality of the data, and the high density of peaks above 2.5 MeV in excitation energy.

In order to determine both the target thickness as well as the optimum choice for the optical potential for the deuterons, elastic scattering data were collected at angles from 15° to 115° in 5° increments.

A. Cross sections and analyzing powers

Cross sections for experiments conducted with the Q3D spectrograph are determined using

$$\frac{d\sigma}{d\Omega}_{\text{lab}}(\theta_{\text{lab}}) = \frac{N(\theta_{\text{lab}})}{N_b\, N_t\, d\Omega\, LT_{\text{DAQ}}\, LT_{\text{Det}}}, \tag{1}$$

where $N(\theta_{\text{lab}})$ is the number of counts in a particular peak; N_b is the number of beam particles incident on the target, as measured by a current integrator connected to a Faraday

cup placed at 0° directly behind the target; N_t is the areal number density of the target; $d\Omega$ is the solid angle subtended by the aperture opening of the Q3D; and $LT_{\rm DAQ}$ and $LT_{\rm Det}$ are the live times of the data acquisition system and the detector, respectively. The solid angle subtended by the spectrograph was determined by slit settings that were calibrated with the elastic scattering data at a given angle.

Taking advantage of the polarized beam that was used during the experiment, the asymmetries in the measured cross sections for the two different beam polarizations were also measured. The analyzing powers, A_y, are given by

$$A_y(\theta) = \left(\frac{2}{3P}\right)\frac{\frac{d\sigma}{d\Omega}_{\uparrow} - \frac{d\sigma}{d\Omega}_{\downarrow}}{\frac{d\sigma}{d\Omega}_{\uparrow} + \frac{d\sigma}{d\Omega}_{\downarrow}}, \tag{2}$$

where P is the polarization of the beam and the subscript arrows refer to cross sections measured with "up" and "down" polarized beam particles, with respect to the beam axis.

Spectroscopic strengths are extracted by comparing the experimental angular distributions of cross sections and analyzing powers with optical model calculations. All quantities were transformed to the center-of-mass frame using the well-known relation

$$\theta_{\rm cm} = \sin^{-1}(\gamma \sin\theta_{\rm lab}) + \theta_{\rm lab}, \tag{3}$$

where the factor γ is

$$\gamma \approx \sqrt{\frac{m_1 m_1'}{m_2 m_2'}\left(\frac{1}{1+\left(1+\frac{m_1}{m_2}\right)\frac{Q}{E}}\right)}, \tag{4}$$

where Q is the reaction Q value to a particular excited state, and E is the energy of the incident particle. The approximation made to obtain the above expression is that the sum of projectile and target masses in the initial state is approximately equal to the sum of the ejectile and residual nuclear mass in the final state; i.e., the Q value is much smaller than the initial total mass. The transformation of the differential cross section can be calculated from the transformation of the scattering angle,

$$\frac{d\sigma}{d\Omega}_{\rm cm} = \frac{d\sigma}{d\Omega}_{\rm lab}\frac{d\Omega_{\rm lab}}{d\Omega_{\rm cm}}, \tag{5}$$

and is

$$\frac{d\sigma}{d\Omega}_{\rm cm} = \frac{d\sigma}{d\Omega}_{\rm lab}\left(\frac{1+\gamma\cos\theta_{\rm cm}}{(1+2\gamma\cos\theta_{\rm cm}+\gamma^2)^{\frac{3}{2}}}\right). \tag{6}$$

Since the analyzing powers are ratios of the difference and sum of cross sections, the center-of-mass analyzing powers are equal to the laboratory-frame analyzing powers. The multiplicative factors that transform the cross sections between the two frames cancel, hence

$$A_y^{\rm lab}(\theta_{\rm lab}) = A_y^{\rm cm}(\theta_{\rm cm}). \tag{7}$$

However, the angular distribution of analyzing powers is slightly different between the two frames, because of the scattering angle transformations.

TABLE I. Deuteron optical model parameters calculated from global optical model potentials; potential well depths are given in MeV, reduced radii and diffuseness parameters are in fm.

Parameter	Daenick *et al.* [38]	Bojowald *et al.* [39]	An and Cai [40]	Han *et al.* [41]
V_{VR}	91.569	90.322	92.840	84.358
r_{VR}	1.170	1.180	1.150	1.174
a_{VR}	0.746	0.804	0.780	0.809
V_{VI}	0.603	0.000	2.472	1.056
r_{VI}	1.325	0.000	1.326	1.563
a_{VI}	0.866	0.000	0.374	0.916
V_{SI}	12.169	12.798	10.157	13.357
r_{SI}	1.325	1.270	1.366	1.328
a_{SI}	0.866	0.869	0.829	0.681
V_{SO}	3.346	3.000	3.557	3.703
r_{SO}	1.070	0.963	0.972	1.234
a_{SO}	0.660	0.963	1.011	0.813
r_C	1.300	1.300	1.303	1.698

B. Elastic scattering data and DWBA calculations

The elastic scattering data collected during the experiment provided the target thickness measurement, and were also used to select the optimal deuteron optical model potential that was used for the distorted wave Born approximation (DWBA) calculations. All DWBA calculations were performed with the code FRESCO [37]. At low angles, the elastic scattering process is dominated by Rutherford scattering and thus the absolute differential cross sections calculated under the DWBA become nearly independent of the choice of optical model potential (OMP). Four different global deuteron OMPs were used in DWBA calculations that were compared with the elastic scattering angular distributions of cross sections and analyzing powers. Tables I and II list the optical potentials used and their respective parameter values. The measured elastic scattering cross sections and analyzing powers are plotted in Fig. 2 along

TABLE II. Proton optical model parameters calculated from global optical model potentials; potential well depths are given in MeV, reduced radii and diffuseness parameters are in fm.

Parameter	Becchetti-Greenlees [42]	Menet *et al.* [43]	Varner *et al.* [44]	Koning-Delaroche [45]
V_{VR}	54.198	52.623	52.186	52.842
r_{VR}	1.170	1.160	1.203	1.220
a_{VR}	0.750	0.750	0.690	0.661
V_{VI}	2.140	3.180	1.238	1.722
r_{VI}	1.320	1.370	1.243	1.266
a_{VI}	0.605	0.564	0.690	0.576
V_{SI}	7.922	5.195	8.439	8.356
r_{SI}	1.320	1.370	1.243	1.266
a_{SI}	0.605	0.564	0.690	0.576
V_{SO}	6.200	6.040	5.900	5.573
r_{SO}	1.010	1.064	1.090	1.051
a_{SO}	0.750	0.780	0.630	0.580
r_C	1.250	1.250	1.262	1.233

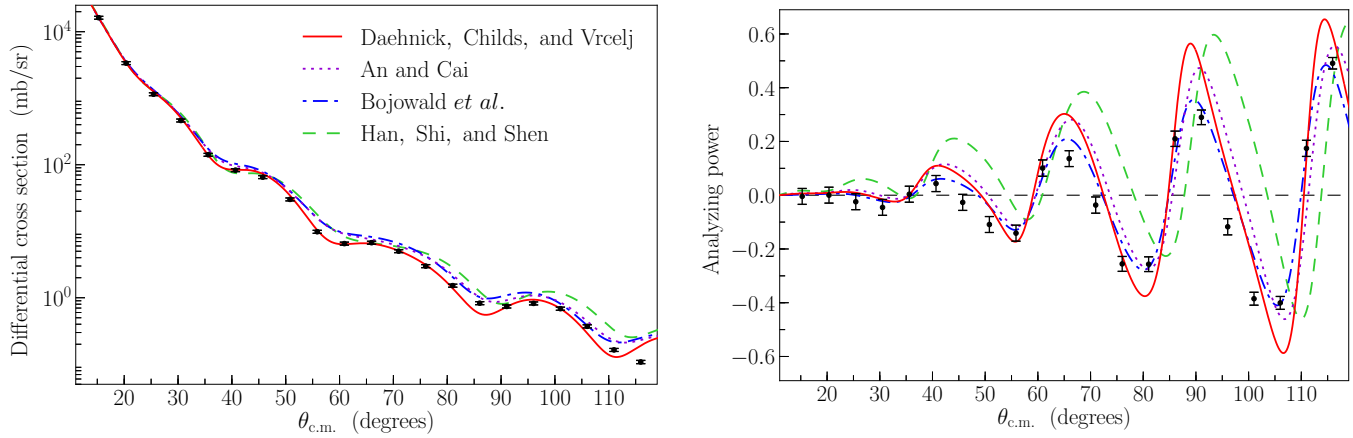

FIG. 2. Measured angular distribution of elastic scattering differential cross section and analyzing powers (points), shown with DWBA calculations with different optical model potentials (curves) of Daehnick, Childs, and Vrcelj [38], An and Chi [40], Bojowald *et al.* [39], and Han, Shi, and Shen [41]. The experimental data have been normalized to match the DWBA cross sections at 15°.

with the optical model calculations. The optical potential that produced the best descriptions of the elastic scattering data was that from Daehnick, Childs, and Vrcelj [38]; this OMP was used in all subsequent calculations.

The lowest scattering angle that was included in the measurement was at 15° in the laboratory frame (15.27° in the center-of-mass frame). The center-of-mass frame experimental cross section at this angle was scaled to the calculated cross section obtained from the optical model calculations, and the target thickness was determined to be $159 \pm 6\ \mu g\,cm^{-2}$.

Since there were no elastic scattering data collected for protons on the residual nucleus, ^{112}Cd, experimental data from the EXFOR database were used to fix the optical potential in the outgoing channel. The proton-^{112}Cd elastic scattering data were taken from Petit *et al.* [46], who used a polarized beam of protons accelerated to 22.3 MeV. Based on both the shape of the angular distribution of cross sections and the shape of the analyzing powers, the optical potential from Koning and Delaroche [45], listed in Table II, was chosen for the outgoing channel potential. The Koning and Delaroche potential was developed for both protons and neutrons, so it was also used in the ADWA calculations for the adiabatic potential in the incoming channel and for the outgoing proton potential.

C. DWBA and ADWA calculations

Spectroscopic strengths were extracted from the observed angular distributions of differential cross section by scaling optical model calculations to the experimental data. Angular distributions from global optical model potentials were calculated with the code FRESCO [37]. As will be seen below, standard DWBA calculations that use a global deuteron potential for the incoming channel and a global proton potential for the outgoing channel were found to deviate from the observed cross sections or analyzing powers of some states, especially those associated with $s_{1/2}$ transfers. To overcome these shortfalls, an alternative approach was tested by using the adiabatic distorted wave approximation (ADWA) (see, e.g., Ref. [47]). Instead of using a global deuteron potential, the sum of a proton potential (V_p) and a neutron potential (V_n) is constructed. The proton and neutron are treated as equally sharing the deuteron's kinetic energy, so the ADWA potential for the deuteron (V_d) at its energy E is [47]

$$V_d(E) = V_p\left(\frac{E}{2}\right) + V_n\left(\frac{E}{2}\right). \tag{8}$$

Both the DWBA and the ADWA analyses are presented and compared below.

The shapes of the angular distributions of cross sections are determined by the dominant ℓ of the transfer, whereas the shapes of the analyzing powers are more sensitive to the dominant j of the transfer [31]. The ^{111}Cd target has $I^\pi = \frac{1}{2}^+$, and, for final state angular momenta with natural parity, the spin-orbit partners $j_<$ and $j_>$ may both contribute to the transfer. In the case of a 2^+ state, for example, the transfer of a neutron into a $2d_{\frac{3}{2}}$ or $2d_{\frac{5}{2}}$ orbital can occur. Since the angular distributions of cross sections for $j_<$ and $j_>$ orbitals are nearly identical, whereas the analyzing powers typically are distinct, the analyzing powers can, in many cases, determine which of these two orbitals dominates the transfer into a given state.

In cases of population of unnatural-parity states, the contributing single particle orbitals for the transferred neutron have distinct ℓ and j values. For 3^+ final states, for example, the cross sections can be dominated by transfers to the $2d_{\frac{5}{2}}$ and $1g_{\frac{7}{2}}$ orbital components of the wave function. It is sometimes the case that both of these single-particle orbitals contribute to the transfer, and the spectroscopic strengths associated with each contribution must be determined simultaneously. However, for most angular distributions observed in this experiment, one clearly dominant single-particle orbital for the transfer was identified.

The spectroscopic strengths were extracted via

$$S_{\ell l} = \frac{\frac{d\sigma}{d\Omega}\big|_{\rm exp}}{\frac{d\sigma}{d\Omega}\big|_{\rm DWBA}}, \tag{9}$$

i.e., by scaling the angular distributions of cross sections from FRESCO to the experimental data. The scaling was done by performing a χ^2 minimization that included data from all

TABLE III. Deuteron adiabatic optical model parameters calculated from the Koning and Delaroche global nucleon optical model potential [45]; potential well depths are given in MeV, and reduced radii and diffuseness parameters are in fm.

Parameter	Proton	Neutron	Parameter	Proton	Neutron
V_{VR}	57.666	51.588	V_{SI}	8.760	8.863
r_{VR}	1.220	1.220	r_{SI}	1.266	1.266
a_{VR}	0.661	0.661	a_{SI}	0.577	0.563
V_{VI}	0.706	0.732	V_{SO}	5.863	5.826
r_{VI}	1.266	1.220	r_{SO}	1.051	1.051
a_{VI}	0.577	0.661	a_{SO}	0.590	0.590
			r_C	1.233	0.000

angles measured. For states with two possible ℓ contributions, the minimization with respect to the cross section data is sufficient for determining the two spectroscopic strengths. For states with a single ℓ but two possible j values, minimization with respect to the analyzing powers is required. The angular distribution of analyzing powers for states with multiple j-transfers is the weighted average of each single-particle orbital contribution,

$$A_y^{\text{total}} = \frac{\sum A_y^{\ell j} S_{\ell j} \frac{d\sigma}{d\Omega}\big|_{\ell j}}{\sum S_{\ell j} \frac{d\sigma}{d\Omega}\big|_{\ell j}}, \tag{10}$$

where $A_y^{\ell j}$, $\frac{d\sigma}{d\Omega}|_{\ell j}$, and $S_{\ell j}$ are the analyzing powers, differential cross sections, and spectroscopic strengths of the (ℓ, j) single-particle configuration. From the results of the minimization, one of the two possible contributions was typically revealed to be dominant.

In general, the OMPs are dependant on the scattering particle's energy. This energy was constant for the incoming deuterons, at 22 MeV. The parameters used in the DWBA calculations for the transfer reaction were the same as those given in Table I for the Daehnick, Childs and Vrcelj potential. The parameters used for the incoming channel in the ADWA calculations were from the Koning and Delaroche optical potential for both protons and neutrons. The potential was evaluated at half the incoming deuteron energy, 11 MeV, and the values are shown in Table III. The outgoing protons had an energy of

$$E_p = E_d + Q - E_{\text{ex}}, \tag{11}$$

where E_d is the energy of the incoming deuteron, Q is the reaction Q value (for the transfer into the ground state, $Q = 7.17$ MeV), and E_{ex} is the excitation energy of the state populated by the transferred neutron. Since the energy of the outgoing proton varies with the excitation energy of the populated state, the optical model parameters from the Koning and Delaroche potential in the outgoing channel were recalculated for each observed state.

III. RESULTS

The spectra collected during the experiment had full-width-at-half-maximum energy resolutions of 6–7 keV. The high-resolution data enabled the identification of 129 levels populated in ^{112}Cd. The angular distributions and analyzing powers, in most cases, were dominated by a single ℓ and j component. In cases where the levels were previously observed [18,48], the spin-parity of the observed level could be verified, and in some cases firmly established. For previously unobserved levels, it was not always possible to assign a spin-parity value. For example, previously unobserved levels demonstrating a dominant $d_{\frac{3}{2}}$ contribution could be either 1^+ or 2^+. The convention chosen for the spectroscopic strengths in Eq. (9) was such that they do not depend on the spin of the final state. In some cases, multiple single-particle contributions were observed for a single level, and both contributions have spectroscopic strengths reported below. Of the 129 level populated, 49 were newly observed.

A. Angular distributions

Angular distributions of cross sections and analyzing powers measured in the current work exhibit the characteristic diffraction pattern oscillations that are typical of general nuclear scattering experiments. The distinct shapes allow for the dominant ℓ and j transfer values to be identified by comparing to the DWBA and ADWA calculations performed with FRESCO.

The high- and low-momentum bite spectra have eight states in common, and these enable a consistency check of the measured absolute cross section. Specifically, the systematic uncertainties associated with dead time corrections and beam current integration could be investigated, and it was found that the uncertainty associated with these measurements was $\approx$1%. Another overall systematic effect is due to target thickness. However, as the target thickness is estimated from the elastic-scattering data obtained with the same experimental setup, in essence the transfer cross sections reported here are normalized relative to the elastic cross section. A conservative estimate of the uncertainty on the transfer cross sections due to normalization procedures is 5%. This systematic uncertainty was used to inflate the errors of the measured cross sections.

The angular distributions for states up to 2.7 MeV observed in the present measurement are plotted in Figs. 3 and 4 along with the DWBA and ADWA calculations used to identify the ℓ and j of the transfer, and extract the spectroscopic strength. The remaining angular distributions are available in the Supplemental Material [49]. The angular distributions calculated from the ADWA potential were generally found to reproduce the experimental data better than the DWBA calculations, especially for low excitation energies. For $0 \leqslant \ell \leqslant 3$, the ADWA calculations have an larger cross section at forward angles than the DWBA predictions, whereas for $\ell > 3$ the opposite is true. This trend is reflected in the experimental data for most states. Neither calculation reproduces the observed analyzing powers, although in many cases the DWBA predictions appear to do slightly better.

B. Spectroscopic strengths

The measured spectroscopic strengths were obtained according to Eq. (9), by scaling the calculated single-particle cross sections to the experimental data. Spectroscopic

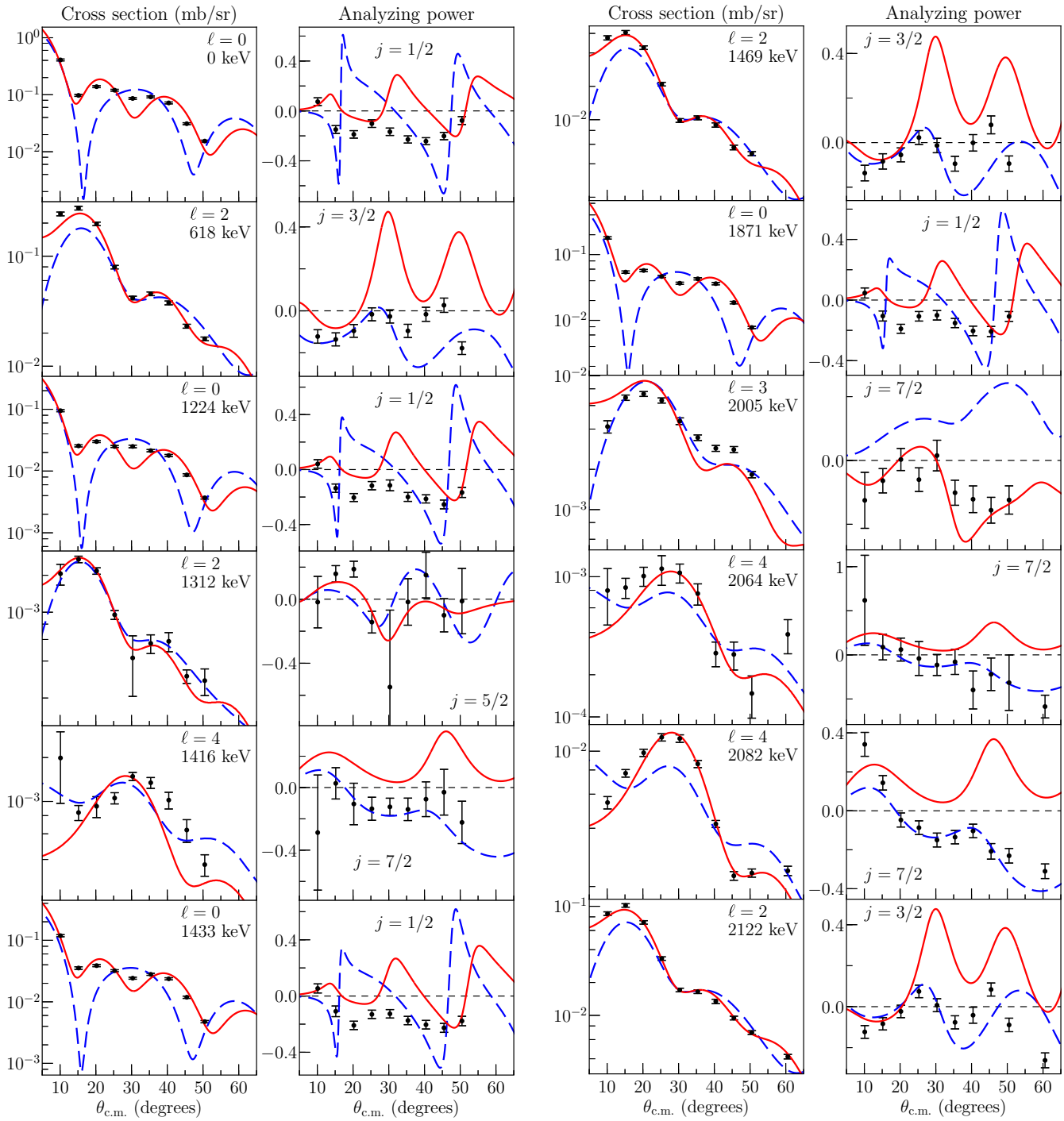

FIG. 3. Angular distributions of differential cross section and analyzing powers of protons from the ^{111}Cd($\vec{d}$, p)^{112}Cd reaction with 22 MeV deuterons for states observed below 2150 keV in excitation energy in ^{112}Cd. Red solid curves are the ADWA calculations, blue dashed curves are DWBA calculations as described in the text. The plots are labeled with the deduced transferred ℓ and j values, as well as the excitation energies of the final states.

strengths were extracted for both the ADWA and DWBA calculations. Comparisons between different OMP sets allowed the assessment of systematic uncertainties associated with choice of parameter sets. Comparisons between the ADWA and DWBA spectroscopic strengths enable an estimate of the uncertainty associated with the choice of the reaction model. Calculations from all 16 pairs of the 4 deuteron and 4 proton parameter sets were performed and used to assess the average and maximum differences in spectroscopic strengths obtained for DWBA calculations. For the strongly populated states, the differences were on average approximately 20%, and the maximum differences were as high as 32%. The OMPs used to extract spectroscopic strengths in the current work were found to be closer to the average values than to

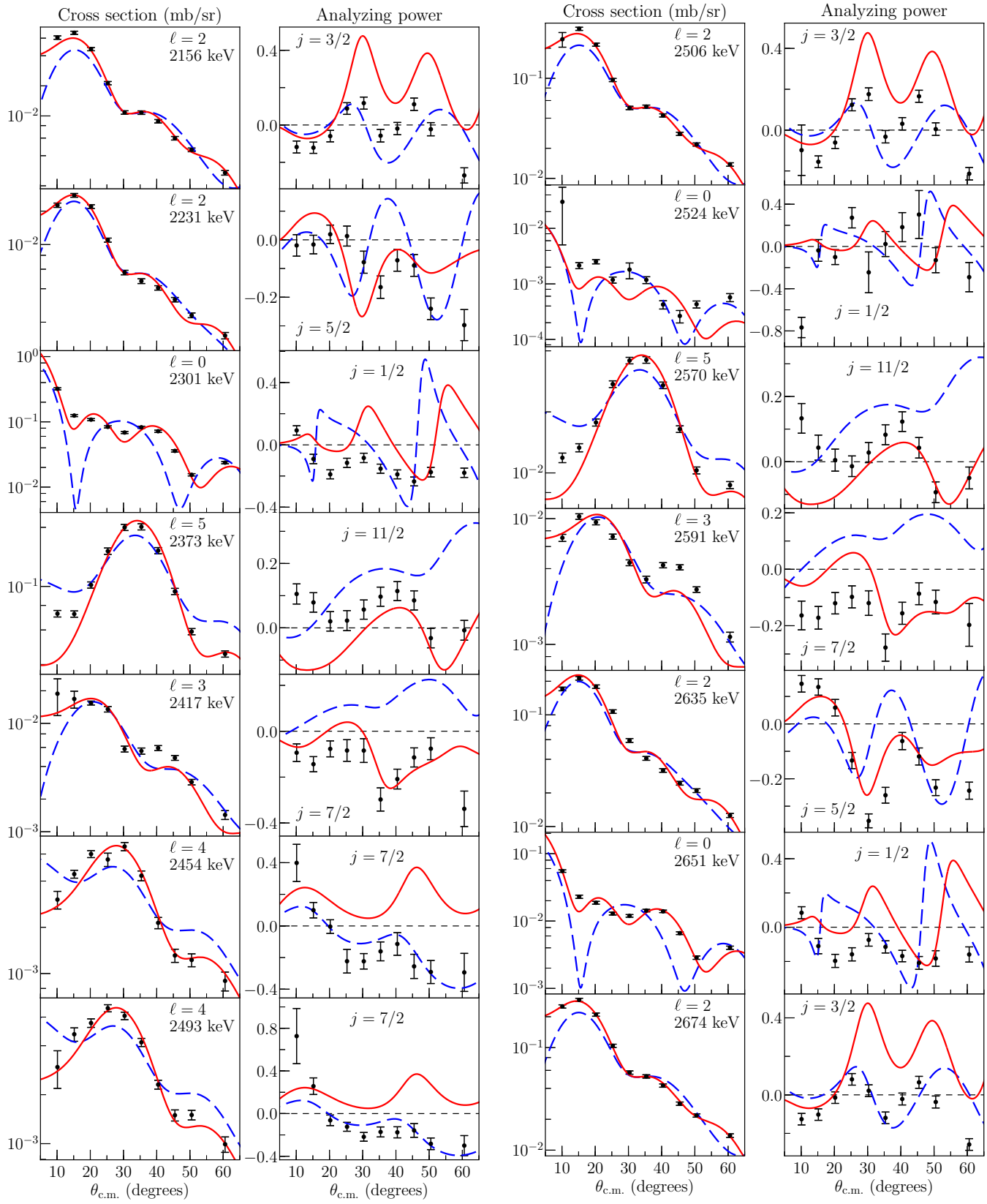

FIG. 4. Angular distributions of differential cross section and analyzing powers of protons from the ^{111}Cd($\vec{d}$, p)^{112}Cd reaction with 22 MeV deuterons for states observed between 2150 and 2700 keV excitation energy in ^{112}Cd. See caption to Fig. 3. The angular distributions for the 103 states analyzed above 2.7 MeV are available in the Supplemental Material [49].

the maximum or minimum values of spectroscopic strengths from all considered OMPs. Differences between the DWBA and ADWA calculations were on average 15%, although in some cases they were as large as 40%. It is further noted that the difference in strengths extracted between the two reaction models exhibits an ℓ dependence, with the high ℓ transfer strengths showing a much greater difference than low ℓ transfers. The average difference of 20% in the strengths resulting from the choice of the OMP is assumed for the strengths extracted from both the DWBA and ADWA comparisons. Table IV lists the spectroscopic strengths for all of the observed levels. The uncertainties reported on the strengths are the statistical uncertainties from the experimental cross sections and the scaling, and the systematic uncertainty associated with the target thickness. An additional 30% systematic uncertainty from the choice of OMP and reaction model is assumed to apply for the spectroscopic strengths reported in Table IV.

C. Discussion of individual states populated

In the subsections below, peaks below approximately 3.2 MeV excitation energy that are newly observed, represent a doublet of states, or for which the angular distributions result in a new spin assignment, are discussed.

1. 1871 keV levels

A doublet of levels is known at an energy of 1871 keV with $I^\pi = 0^+$ and 4^+. A level at 1871.33(11) keV was observed in the current work dominated by an $\ell = 0$ transfer, consistent with $I^\pi = 0^+$. This level had a spectroscopic strength of about half the value of the ground state transfer. This result is consistent with the previous (d, p) study by Barnes *et al.* [29]. The $I^\pi = 4^+$ level may be weakly populated in this reaction, although the angular distributions of cross sections and analyzing powers showed no characteristics deviating from that expected for $s_{\frac{1}{2}}$ transfer.

2. 2501 keV level, unobserved

The $(\vec{d}, t)$ study by Blasi *et al.* [28] identified a weak $\ell = 0$ transfer to a level at 2501 keV. This level was not observed in the $(n, n'\gamma)$ study by Garrett *et al.* [18], and was interpreted as an impurity, most likely from the transfer to the ground state from the ^{113}Cd$(\vec{d}, t)^{114}$Cd reaction. A level consistent with an energy of 2501 keV was not observed in the current work; however, if it was weakly populated, it would be unresolvable from the strongly populated $J = 2^+$ level at 2506 keV.

3. 2507 keV levels

A doublet of levels has been suggested at 2507 keV. A $I^\pi = 1^-$ level at 2506.53(9) and a spin 4 or 5 level at 2506.88(7) keV were proposed by Délèze *et al.* [50]. The latter was was ruled out by Garrett *et al.* [18], but they proposed a doublet of levels with $I^\pi = 1^-$ at 2506.733(23) and a $I^\pi = 2^+$ level at 2506.337(22). In the current work, a level was observed at 2506.10(6) keV dominated by a $d_{\frac{3}{2}}$ transfer, consistent with the 2^+ assignment. There was no evidence for population of an $I^\pi = 1^-$ state, but this would be very weakly populated in the (d, p) reaction since it would require $p_{\frac{1}{2}}$ or $p_{\frac{3}{2}}$ transfer strength, and these orbitals are far below the Fermi surface.

4. 2524 keV level

A weakly populated state was observed in the current work at 2524 keV for which a $s_{\frac{1}{2}}$ transfer was measured, consistent with $I^\pi = 0^+$. This level was not observed in previous $(\vec{d}, t)$ [28] or $(n, n'\gamma)$ [18] studies of ^{112}Cd. Since this level is a low spin level below 3.2 MeV, it is highly unlikely that it would have remained undetected in the $(n, n'\gamma)$ study, and it is therefore suggested to result from a target impurity. However, comparing the energy of the level with known levels that are strongly populated in nearby isotopes, none of them were found to be candidates. While the existence of a new level at 2524 keV is doubtful, no explanation for a peak at this energy can be given.

5. 2793.5 keV level

A peak dominated by a $g_{\frac{7}{2}}$ transfer corresponding to an excitation energy of 2793.5(4) keV was observed [49], which would imply a previously unobserved level. This level would possess $I^\pi = 3^+$ or 4^+ and thus it is unlikely that it would have remained undetected in the $(n, n'\gamma)$ study [18]. Since the cross section is very small, it is suggested to be the result of a target impurity, although no observed levels in nearby isotopes are consistent with the energy.

6. 2817.7 keV levels

Previous studies have demonstrated the existence of a $I^\pi = 6^-$ level at 2818 keV. A level dominated by an $h_{\frac{11}{2}}$ transfer was observed [49] in the current work at 2817.74(6) keV. This state had the largest spectroscopic strength of any peak observed in the spectrum. The $I^\pi = 4^+$ level observed by Garrett *et al.* [18] at 2816 keV was not observed, but would have been difficult to identify due to the strongly populated 6^- level.

7. 2852.8 keV level

In the $(\vec{d}, t)$ study by Blasi *et al.* [28], an $I^\pi = 0^+$ level at 2853 keV was observed. The $(n, n'\gamma)$ study by Garrett *et al.* [18] observed a level consistent with this energy, but assigned it unambiguously as $I^\pi = 2^+$ from the angular distribution of a ground state transition. It was suggested by Garrett *et al.* that the 0^+ level from the $(\vec{d}, t)$ experiment could be an impurity from the ^{112}Cd$(\vec{d}, t)^{111}$Cd transfer into the ground state. The difference in Q value from the ^{113}Cd$(\vec{d}, t)^{112}$Cd reaction is 2856 keV, which is not quite the energy measured by Blasi *et al.* [28], but is consistent within uncertainties. However, the observation of an $\ell = 0$ transfer into a level at 2852.8(2) keV observed in the current work [49] agrees unambiguously with both the energy and spin-parity assignment in the $(\vec{d}, t)$ work [28]. This suggests the presence of a doublet of states at 2853 keV, with the 0^+ level undetected in the $(n, n'\gamma)$ study. There is some evidence of the $I^\pi = 2^+$ level in both

TABLE IV. Measured excitation energies, cross sections, spin-parity values, and spectroscopic strengths for levels observed in the ^{111}Cd$(\vec{d}, p)^{112}$Cd reaction. Levels used for calibration are indicated in column 3, using the values listed in column 1 that are taken from Ref. [18]. The reported differential cross sections are taken from the data at 30°. For the $(\vec{d}, p)$ reaction data, a transfer listed as $\ell_{(j)}$ indicates that the dominant transfer is ℓ_j, but for which the spin-orbit partner cannot be excluded. Uncertainties on all quantities are statistical only; uncertainties in the spectroscopic strengths include the statistical contribution and the target thickness systematic uncertainty, and do not include the overall 30% systematic uncertainty due to OMP and reaction model choice. The final column reproduces the data from Ref. [28] for ease of comparison; j values in parenthesis indicate a multiple ℓ-component fit in Ref. [28]. Only those levels and $S_{\ell j}$ values for the largest strengths that correspond to the presently observed results are listed.

Literature		^{111}Cd$(\vec{d}, p)$						^{113}Cd$(\vec{d}, t)$			
E (keV)	I^π	E (keV)	I^π	$\frac{d\sigma}{d\Omega}_{\rm cm}$ (mb/sr)	ℓ_j	$S_{\ell j}^{\rm ADWA}$	$S_{\ell j}^{\rm DWBA}$	E (keV)	I^π	ℓ_j	$S_{\ell j}$
GS	0^+	GS[a]	0^+	0.086(3)	$s_{\frac{1}{2}}$	0.185(2)	0.189(3)	GS	0^+	$s_{\frac{1}{2}}$	1.140
617.520(11)	2^+	617.59(9)[a]	2^+	0.042(2)	$d_{(\frac{3}{2})}$	0.256(3)	0.185(2)	618	2^+	$d_{\frac{5}{2}}$	0.374
1224.41(2)	0^+	1224.13(10)[a]	0^+	0.025(1)	$s_{\frac{1}{2}}$	0.0437(6)	0.0463(7)				
1312.393(8)	2^+	1312.3(3)[a]	2^+	0.0004(2)	$d_{(\frac{5}{2})}$	0.00230(8)	0.00244(8)	1314	2^+	$d_{\frac{5}{2}}$	0.134
1415.561(16)	4^+	1415.6(3)[a]	4^+	0.00149(10)	$g_{\frac{7}{2}}$	0.0166(6)	0.0140(5)	1417	4^+	$g_{\frac{7}{2}}$	0.169
1433.30(2)	0^+	1433.37(10)[a]	0^+	0.0242(9)	$s_{\frac{1}{2}}$	0.0579(8)	0.0493(8)				
1468.835(10)	2^+	1469.05(11)[a]	2^+	0.0098(4)	$d_{(\frac{3}{2})}$	0.0611(8)	0.0446(6)	1470	2^+	$d_{(\frac{3}{2})}$	0.013
1871.2(4)	0^+	1871.33(11)	0^+	0.037(1)	$s_{\frac{1}{2}}$	0.0876(12)	0.0736(12)	1872	0^+	$s_{\frac{1}{2}}$	0.025
2005.189(16)	3^-	2005.15(9)[a]	3^-	0.0046(2)	$f_{\frac{7}{2}}$	0.0126(2)	0.0119(18)	2005	3^-	$f_{\frac{7}{2}}$	0.014
2064.51(2)	3^+	2064.3(3)[a]	3^+	0.0011(2)	$g_{\frac{7}{2}}$	0.0129(9)	0.0083(6)	2065	3^+	$d_{\frac{5}{2}}$	0.009
2081.715(16)	4^+	2081.70(9)[a]	4^+	0.0116(5)	$g_{\frac{7}{2}}$	0.146(2)	0.085(13)	2082	4^+	$g_{\frac{7}{2}}$	0.093
2121.530(19)	2^+	2121.53(5)[a]	2^+	0.0171(6)	$d_{(\frac{3}{2})}$	0.0971(12)	0.0694(9)	2121	2^+	$d_{\frac{3}{2}}$	0.012
2156.18(2)	2^+	2156.22(5)[a]	2^+	0.0108(4)	$d_{(\frac{3}{2})}$	0.0629(8)	0.0446(6)	2155	2^+	$d_{(\frac{3}{2})}$	0.012
2231.20(2)	2^+	2231.11(6)[a]	2^+	0.0056(3)	$d_{(\frac{5}{2})}$	0.0242(4)	0.0219(3)	2230	2^+	$d_{\frac{3}{2}}$	0.006
2300.74(3)	0^+	2300.90(4)	0^+	0.069(3)	$s_{\frac{1}{2}}$	0.1670(2)	0.132(18)	2299	0^+	$s_{\frac{1}{2}}$	0.133
2373.28(2)	5^-	2373.28(3)[a]	5^-	0.200(7)	$h_{\frac{11}{2}}$	2.66(3)	1.59(19)	2372	5^-	$h_{\frac{11}{2}}$	0.232
2416.00(6)	3^-	2416.72(16)	3^-	0.0058(4)	$f_{\frac{7}{2}}$	0.0264(4)	0.0166(3)	2414	$3,4^-$	$f_{\frac{7}{2}}$	0.006
2454.52(6)	4^+	2454.16(15)	4^+	0.0067(4)	$g_{\frac{7}{2}}$	0.0800(2)	0.048(12)	2453	$3,4^+$	$g_{\frac{7}{2}}$	0.110
2493.163(11)	4^+	2492.8(4)[a]	4^+	0.0061(3)	$g_{\frac{7}{2}}$	0.0767(17)	0.0508(11)	2491	$3,4^+$	$g_{\frac{7}{2}}$	0.054
2506.33(2)	2^+	2506.10(6)	2^+	0.051(2)	$d_{(\frac{3}{2})}$	0.291(4)	0.201(3)	2505	2^+	$d_{(\frac{3}{2})}$	0.034
		2524.1(11)[b]	0^+	0.0018(6)	$s_{\frac{1}{2}}$	0.00180(10)	0.00223(12)				
2570.29(3)	5^-	2570.23(7)	5^-	0.036(1)	$h_{\frac{11}{2}}$	0.468(6)	0.284(4)	2569	$5,6^-$	$h_{\frac{11}{2}}$	0.098
2591.046(14)	4^-	2591.11(9)[a]	4^-	0.0045(2)	$f_{\frac{7}{2}}$	0.0167(3)	0.0106(18)	2589	$3,4^-$	$f_{\frac{7}{2}}$	0.005
2634.996(16)	3^+	2635.28(4)	3^+	0.059(2)	$d_{(\frac{5}{2})}$	0.198(2)	0.176(2)	2634	$2,3^+$	$d_{\frac{5}{2}}$	0.440
2650.16(5)	0^+	2650.58(11)	0^+	0.0119(5)	$s_{\frac{1}{2}}$	0.0286(4)	0.0221(4)	2649	0^+	$s_{\frac{1}{2}}$	0.023
2674.02(6)	2^+	2674.08(4)[a]	2^+	0.057(2)	$d_{(\frac{3}{2})}$	0.297(4)	0.208(3)	2673	2^+	$d_{(\frac{3}{2})}$	0.097
2711.3(3)	4^+	2710.94(6)	4^+	0.041(2)	$g_{\frac{7}{2}}$	0.505(7)	0.290(4)	2710	$3,4^+$	$g_{\frac{7}{2}}$	0.372
2723.88(3)	2^+	2723.85(4)[a]	2^+	0.063(2)	$d_{(\frac{5}{2})}$	0.217(3)	0.192(2)	2724	$2,3^+$	$d_{\frac{5}{2}}$	0.407
2765.75(3)	2^+	2765.73(4)[a]	2^+	0.060(2)	$d_{(\frac{3}{2})}$	0.337(4)	0.234(3)	2765	2^+	$d_{(\frac{3}{2})}$	0.057
		2793.5(4)[b]	$3^+, 4^+$	0.0045(3)	$g_{\frac{7}{2}}$	0.0720(2)	0.058(15)	2799	$1,2^+$	$d_{\frac{3}{2}}$	0.012
2817.80(3)	6^-	2817.74(6)	6^-	0.47(2)	$h_{\frac{11}{2}}$	6.07(7)	3.47(4)	2818	$1,2^+$ $5,6^-$	$d_{\frac{3}{2}}$ $h_{\frac{11}{2}}$	0.038 0.562
2834.43(7)	0^+	2834.62(7)	0^+	0.061(2)	$s_{\frac{1}{2}}$	0.1451(19)	0.1152(17)	2834	0^+	$s_{\frac{1}{2}}$	0.032
2853	0^+[c]	2852.8(2)	0^+	0.0178(8)	$s_{\frac{1}{2}}$	0.0418(6)	0.0343(6)	2853	0^+	$s_{\frac{1}{2}}$	0.004
2866.86(2)	3^-	2867.94(8)	3	0.099(4)	$f_{\frac{5}{2}}$	0.017(2)	0.042(3)				
2867.48(7)	(3^+)		3^+		$g_{\frac{7}{2}}$	0.538(2)	0.277(4)	2868	3^+	$(g_{\frac{7}{2}})$	0.648
2882.74(5)	0^+	2882.67(17)	0^+	0.0137(9)	$s_{\frac{1}{2}}$	0.0362(8)	0.0274(7)	2882	0^+	$s_{\frac{1}{2}}$	0.015
2893.58(5)	4^+	2893.0(5)[a]	4^+	0.028(7)	$g_{\frac{7}{2}}$	0.360(2)	0.18(10)	2894	$3,4^+$	$g_{\frac{7}{2}}$	0.446
2899.09(6)	(5^-)	2899.01(11)	5^-	0.096(8)	$h_{\frac{11}{2}}$	1.200(3)	0.78(16)				
2924.83(3)	4^-	2924.5(3)	4^-	0.014(2)	$f_{\frac{7}{2}}$	0.0554(16)	0.0329(10)				
2931.51(5)	1^+	2931.62(8)[a]	1^+	0.028(2)	$d_{(\frac{3}{2})}$	0.144(2)	0.108(18)	2931	$1,2^+$	$d_{\frac{3}{2}}$	0.014
		2946.98(8)[b]	$3^-, 4^-$	0.029(1)	$f_{\frac{7}{2}}$	0.1192(16)	0.0692(9)	2946	$2,3^+$ $3,4^+$	$d_{\frac{5}{2}}$ $g_{\frac{7}{2}}$	0.019 0.060
2961.93(3)	4^-	2961.89(7)	4^-	0.048(2)	$f_{\frac{7}{2}}$	0.180(2)	0.104(13)	2960	4^-	$f_{(\frac{7}{2})}$	0.012

TABLE IV. (*Continued.*)

Literature		^{111}Cd($\vec{d}$, p)						^{113}Cd($\vec{d}$, t)			
E (keV)	I^π	E (keV)	I^π	$\frac{d\sigma}{d\Omega\,\mathrm{cm}}$ (mb/sr)	ℓ_j	$S_{\ell j}^{\mathrm{ADWA}}$	$S_{\ell j}^{\mathrm{DWBA}}$	E (keV)	I^π	ℓ_j	$S_{\ell j}$
2980.82(3)	2^+	2980.88(6)[a]	2^+	0.0184(8)	$d_{(\frac{3}{2})}$	0.0850(12)	0.0596(9)	2980	2^+	$d_{(\frac{3}{2})}$	0.013
3002.13(2)	(3^+)	3002.2(4)[a]	3^+	0.017(3)	$g_{\frac{7}{2}}$	0.226(6)	0.146(4)	3001	(3^+)	$(g_{\frac{7}{2}})$	0.062
3049.23(6)	(1^-)[c]	3049.1(2)[a]	1^-	0.0047(3)	$p_{\frac{3}{2}}$	0.00442(15)	0.00363(12)				
		3067.10(10)	0^+	0.038(2)	$s_{\frac{1}{2}}$	0.0918(16)	0.0655(13)				
3071.28(8)	$(1,2)^+$	3073.7(3)	$1^+, 2^+$	0.018(1)	$d_{(\frac{3}{2})}$	0.0720(2)	0.053(16)	3069	$\begin{cases}1,2^+\\3,4^+\end{cases}$	$d_{\frac{3}{2}}$ $g_{\frac{7}{2}}$	0.016 0.043
3105.61(5)	(2),3	3107.9(3)	2^-	0.132(9)	$p_{\frac{3}{2}}$	0.126(4)	0.138(4)				
3109.86(6)	1	3111.6(3)	1^+	0.123(9)	$d_{(\frac{3}{2})}$	0.829(16)	0.546(11)	3109	2^+	$d_{(\frac{3}{2})}$	0.099
3131(1)	3^-[c]	3130.1(2)	3^-	0.030(1)	$f_{\frac{7}{2}}$	0.1004(14)	0.0599(8)				
3145.39(5)	4^+	3144.5(5)	4^+	0.018(2)	$g_{\frac{7}{2}}$	0.210(8)	0.138(6)	3146	4^+	$g_{\frac{7}{2}}$	0.156
		3151.6(3)	$1^+, 2^+$	0.020(2)	$d_{(\frac{3}{2})}$	0.0892(20)	0.0682(15)				
3169.56(3)	2^+	3168.9(3)	$\begin{cases}2^+, 3^+\\2^-, 3^-\end{cases}$	0.0135(10)	$d_{(\frac{5}{2})}$ $f_{\frac{5}{2}}$	0.008(2) 0.020(2)	0.006(2) 0.022(2)				
3178.80(6)	2^+	3178.79(4)[a]	2^+	0.103(4)	$d_{(\frac{3}{2})}$	0.505(6)	0.350(4)	3177	$\begin{cases}1,2^+\\3,4^+\end{cases}$	$d_{\frac{3}{2}}$ $g_{\frac{7}{2}}$	0.032 0.079
3194.50(8)	2^+, (3^+)	3194.40(14)[a]	2^+	0.025(1)	$d_{(\frac{3}{2})}$	0.133(2)	0.088(16)	3194	2^+	$d_{(\frac{3}{2})}$	0.073
3203.25(11)	$3^{(+)}$	3202.8(4)	3^+	0.022(1)	$\begin{cases}d_{(\frac{5}{2})}\\g_{\frac{7}{2}}\end{cases}$	0.002(1) 0.11(1)	0.003(1) 0.12(2)	3204	(3^+)	$d_{\frac{5}{2}}$ $g_{\frac{7}{2}}$	0.014 0.176
3231.41(5)	1^+	3231.77(6)	1^+	0.043(2)	$d_{(\frac{3}{2})}$	0.226(3)	0.159(2)	3230	$1,2^+$	$d_{\frac{3}{2}}$	0.026
3242.59(8)	2^+	3243.04(15)	2^+	0.0169(9)	$d_{(\frac{3}{2})}$	0.0861(14)	0.0623(10)	3242	2^+	$d_{(\frac{5}{2})}$	0.013
3251.86(17)	0^+	3252.35(14)	0^+	0.020(1)	$s_{\frac{1}{2}}$	0.0465(8)	0.0360(7)	3252	$\begin{cases}0^+\\3^+\end{cases}$	$s_{\frac{1}{2}}$ $g_{(\frac{7}{2})}$	0.002 0.033
3266.61(4)	3–5	3266.06(18)	2-4$^+$	0.0195(8)	$\begin{cases}d_{(\frac{5}{2})}\\g_{\frac{7}{2}}\end{cases}$	0.0013(2) 0.110(3)	0.0022(3) 0.118(5)				
3291.16(5)		3291.4(4)	$3^+, 4^+$	0.010(1)	$g_{\frac{7}{2}}$	0.170(6)	0.112(4)				
3301.0(2)	1	3300.27(11)	1^+	0.045(2)	$d_{(\frac{3}{2})}$	0.214(3)	0.149(2)	3296	2^+	$d_{(\frac{5}{2})}$	0.114
3312.19(4)	1–3	3313.5(3)	3^+	0.0125(7)	$g_{\frac{7}{2}}$	0.151(4)	0.095(2)	3312	$\begin{cases}1,2^+\\5,6^-\end{cases}$	$d_{\frac{3}{2}}$ $h_{\frac{11}{2}}$	0.014 0.090
3332.04(3)	3–5	3331.5(2)	2-4$^+$	0.020(1)	$\begin{cases}d_{(\frac{5}{2})}\\g_{\frac{7}{2}}\end{cases}$	0.0037(3) 0.103(4)	0.0056(5) 0.113(6)	3330	$2,3^+$	$d_{\frac{5}{2}}$	0.051
		3342.06(8)	$1^+, 2^+$	0.048(2)	$d_{(\frac{3}{2})}$	0.254(3)	0.171(2)	3340	2^+	$d_{(\frac{3}{2})}$	0.035
3363.59(6)	2^+	3363.07(15)	2^+	0.0134(7)	$d_{(\frac{3}{2})}$	0.0615(10)	0.0462(7)	3361	2^+	$d_{(\frac{3}{2})}$	0.023
		3375.9(2)	$3^-, 4^-$	0.011(1)	$f_{\frac{7}{2}}$	0.0391(11)	0.0236(6)				
3383.63(5)	(3)	3383.7(2)[a]	3^+	0.006(1)	$d_{(\frac{5}{2})}$	0.0324(10)	0.0272(8)	3381	2^+	$d_{(\frac{3}{2})}$	0.004
3402.93(7)	3^+	3404.1(2)	2-4$^+$	0.025(1)	$\begin{cases}d_{(\frac{5}{2})}\\g_{\frac{7}{2}}\end{cases}$	0.0057(3) 0.123(5)	0.0090(6) 0.134(7)	3402	$2,3^+$	$d_{\frac{5}{2}}$	0.050
3422.6(2)	0–4	3423.3(3)	0^+	0.017(1)	$s_{\frac{1}{2}}$	0.0413(12)	0.0286(9)	3422	$\begin{cases}0^+\\1,2^+\end{cases}$	$s_{\frac{1}{2}}$ $d_{\frac{3}{2}}$	0.005 0.007
3433.80(8)	3–5	3432.3(4)	3^+	0.057(2)	$d_{(\frac{5}{2})}$	0.203(4)	0.165(3)	3433	$\begin{cases}0^+\\1,2^+\end{cases}$	$s_{\frac{1}{2}}$ $d_{\frac{3}{2}}$	0.004 0.020
		3437.5(8)	$1^+, 2^+$	0.017(1)	$d_{(\frac{3}{2})}$	0.0750(3)	0.044(18)				
3452.89(11)	3^+,(2)	3450.5(4)	3^+	0.0094(8)	$g_{\frac{7}{2}}$	0.146(5)	0.092(3)				
3471.4(3)		3471.8(4)	$3^+, 4^+$	0.0136(9)	$g_{\frac{7}{2}}$	0.181(6)	0.126(4)				
		3480.3(3)	$1^+, 2^+$	0.026(1)	$d_{(\frac{3}{2})}$	0.120(2)	0.084(15)				
		3488.9(3)	$1^+, 2^+$	0.015(1)	$d_{(\frac{3}{2})}$	0.0746(17)	0.0512(12)				
		3513.2(2)	0^+	0.0134(8)	$s_{\frac{1}{2}}$	0.0262(6)	0.0228(5)				
3522.51(4)	1–3	3522.9(2)	2^+	0.0108(7)	$d_{(\frac{3}{2})}$	0.0476(11)	0.0342(8)				
		3533.1(2)	$1^+, 2^+$	0.024(1)	$d_{(\frac{3}{2})}$	0.0897(15)	0.0639(10)				
		3544.8(5)	$5^-, 6^-$	0.0052(6)	$h_{\frac{11}{2}}$	0.0250(3)	0.018(18)				
3557.33(4)	1–3	3557.07(19)	0^+	0.039(2)	$s_{\frac{1}{2}}$	0.0909(13)	0.0690(11)				

TABLE IV. (*Continued.*)

Literature		^{111}Cd($\vec{d}$, p)						^{113}Cd($\vec{d}$, t)			
E (keV)	I^π	E (keV)	I^π	$\frac{d\sigma}{d\Omega_{\rm cm}}$ (mb/sr)	ℓ_j	$S_{\ell j}^{\rm ADWA}$	$S_{\ell j}^{\rm DWBA}$	E (keV)	I^π	ℓ_j	$S_{\ell j}$
3568.05(6)	2^+	3568.3(4)	2^+	0.0086(6)	$d_{(\frac{3}{2})}$	0.0410(9)	0.0294(7)				
		3581.3(9)	$1^-, 2^-$	0.0023(4)	$p_{\frac{3}{2}}$	0.00194(17)	0.00158(14)				
		3596.6(2)	0^+	0.0155(7)	$s_{\frac{1}{2}}$	0.0378(6)	0.0284(5)				
		3612.1(2)	$1^+, 2^+$	0.029(1)	$d_{(\frac{3}{2})}$	0.1359(18)	0.0911(12)				
		3626.6(3)	$2^+, 3^+$	0.0123(7)	$d_{(\frac{5}{2})}$	0.0040(2)	0.00560(5)				
3627.7(3)	4–6		$5^-, 6^-$		$h_{\frac{11}{2}}$	0.068(3)	0.076(3)				
3652.16(7)	1	3649.9(3)	1^+	0.0136(6)	$d_{(\frac{3}{2})}$	0.0448(8)	0.0349(6)				
3665.78(4)	3,(2)	3665.4(3)	$2^+, 3^+$	0.0167(7)	$d_{(\frac{5}{2})}$	0.0455(7)	0.0393(6)				
		3682.4(3)	0^+	0.0133(6)	$s_{\frac{1}{2}}$	0.0254(5)	0.0226(4)				
3697.69(14)	2–4	3695.7(7)	$2^+, 3^+$	0.0055(6)	$d_{(\frac{5}{2})}$	0.0106(6)	0.0097(5)				
		3703.6(3)	0^+	0.037(2)	$s_{\frac{1}{2}}$	0.0856(13)	0.0690(12)				
3720.7(3)	2–6	3719.7(3)	$2^+, 3^+$	0.031(1)	$d_{(\frac{5}{2})}$	0.0771(11)	0.0667(9)				
		3737.9(10)	0^+	0.007(1)	$s_{\frac{1}{2}}$	0.0111(5)	0.0121(6)				
		3742.7(8)	$1^+, 2^+$	0.0081(9)	$d_{(\frac{3}{2})}$	0.0439(11)	0.0330(8)				
3755.46(17)	1	3753.0(8)	1^+	0.0057(7)	$d_{(\frac{3}{2})}$	0.0182(7)	0.0136(5)				
		3769.4(8)	$5^-, 6^-$	0.0159(8)	$h_{\frac{11}{2}}$	0.219(4)	0.138(3)				
		3780.3(4)	$1^+, 2^+$	0.036(1)	$d_{(\frac{3}{2})}$	0.156(2)	0.106(14)				
		3794.0(11)	$1^+, 2^+$	0.0011(3)	$d_{(\frac{3}{2})}$	0.0090(5)	0.0062(3)				
3810.88(13)	1–3	3810.2(5)	$2^+, 3^+$	0.0167(8)	$d_{(\frac{5}{2})}$	0.0454(8)	0.0399(7)				
		3819.7(5)	$1^+, 2^+$	0.0087(6)	$d_{(\frac{3}{2})}$	0.0348(8)	0.0250(6)				
3832.66(13)	1–3	3833.9(5)	$1^+, 2^+$	0.0114(6)	$d_{(\frac{3}{2})}$	0.0321(7)	0.0252(6)				
		3843.9(8)	0^+	0.0043(4)	$s_{\frac{1}{2}}$	0.0090(4)	0.0078(4)				
		3868.6(4)	0^+	0.0089(6)	$s_{\frac{1}{2}}$	0.0186(5)	0.0164(4)				
3878.62(16)	1–3	3877.4(5)	3^+	0.0144(8)	$g_{\frac{7}{2}}$	0.209(5)	0.138(3)				
		3887.5(5)	$5^-, 6^-$	0.0148(8)	$h_{\frac{11}{2}}$	0.198(4)	0.121(2)				
		3901.2(8)	$2^+, 3^+$	0.0035(4)	$d_{(\frac{5}{2})}$	0.0082(4)	0.0074(3)				
		3911.2(6)	$2^+, 3^+$	0.0056(5)	$d_{(\frac{5}{2})}$	0.0131(4)	0.0113(3)				
		3923.7(5)	$5^-, 6^-$	0.0176(8)	$h_{\frac{11}{2}}$	0.186(4)	0.118(2)				
3933.08(17)	1	3932.4(6)	1^+	0.0106(6)	$d_{(\frac{3}{2})}$	0.0400(8)	0.0288(6)				
3952.26(6)	1–3	3951.8(6)	2^+	0.030(1)	$d_{(\frac{5}{2})}$	0.0921(12)	0.0748(10)				
		3970.9(8)	$3^+, 4^+$	0.0065(4)	$g_{\frac{7}{2}}$	0.0930(3)	0.059(17)				
		3982.4(7)	$2^+, 3^+$	0.0039(4)	$d_{(\frac{5}{2})}$	0.0132(4)	0.0112(3)				
		4001.0(7)	$2^+, 3^+$	0.0091(5)	$d_{(\frac{5}{2})}$	0.0234(5)	0.0206(4)				
		4018.5(8)	$1^+, 2^+$	0.0039(7)	$d_{(\frac{3}{2})}$	0.0216(8)	0.0155(5)				
		4029.1(9)	$1^+, 2^+$	0.0116(9)	$d_{(\frac{3}{2})}$	0.0479(12)	0.0326(8)				
		4039.4(12)	$1^+, 2^+$	0.0047(7)	$d_{(\frac{3}{2})}$	0.0208(12)	0.0141(8)				
		4048.5(11)	$2^+, 3^+$	0.008(2)	$d_{(\frac{5}{2})}$	0.0233(11)	0.0199(9)				
		4056.1(12)	$2^+, 3^+$	0.007(2)	$d_{(\frac{5}{2})}$	0.0216(11)	0.0183(9)				
		4068.5(17)	$1^+, 2^+$	0.0008(4)	$d_{(\frac{3}{2})}$	0.0071(8)	0.0045(5)				
		4087.2(8)	$2^+, 3^+$	0.0174(8)	$d_{(\frac{5}{2})}$	0.0524(10)	0.0434(8)				
		4096.9(12)	$3^-, 4^-$	0.0044(5)	$f_{\frac{7}{2}}$	0.0120(7)	0.0064(4)				
		4111.4(9)	$2^-, 3^-$	0.031(1)	$f_{\frac{5}{2}}$	0.0126(5)	0.0134(7)				
			$5^-, 6^-$		$h_{\frac{11}{2}}$	0.105(6)	0.126(8)				
		4121.8(12)	$1^+, 2^+$	0.0039(4)	$d_{(\frac{3}{2})}$	0.0117(6)	0.0087(4)				
		4134.6(10)	$3^+, 4^+$	0.0065(5)	$g_{\frac{7}{2}}$	0.0880(3)	0.0564(18)				
		4145.9(9)	0^+	0.0074(5)	$s_{\frac{1}{2}}$	0.0144(4)	0.0130(3)				
		4157.9(9)	$1^+, 2^+$	0.0055(4)	$d_{(\frac{3}{2})}$	0.0181(5)	0.0128(4)				
		4170.4(10)	$2^-, 3^-$	0.0052(4)	$f_{\frac{5}{2}}$	0.0149(4)	0.0110(3)				
		4183.7(11)	$2^+, 3^+$	0.0037(4)	$d_{(\frac{5}{2})}$	0.0081(3)	0.0071(3)				

TABLE IV. (*Continued.*)

Literature		^{111}Cd$(\vec{d}, p)$						^{113}Cd$(\vec{d}, t)$			
E (keV)	I^π	E (keV)	I^π	$\frac{d\sigma}{d\Omega}_{\rm cm}$ (mb/sr)	ℓ_j	$S_{\ell j}^{\rm ADWA}$	$S_{\ell j}^{\rm DWBA}$	E (keV)	I^π	ℓ_j	$S_{\ell j}$
		4207.2(11)	$0^-, 1^-$	0.0068(5)	$p_{\frac{1}{2}}$	0.0079(2)	0.00807(19)				
		4223.1(11)	$5^-, 6^-$	0.0073(5)	$h_{\frac{11}{2}}$	0.104(3)	0.0702(18)				

[a]Used as calibration point.
[b]Existence of level in ^{112}Cd is doubtful, but no target impurity responsible for the peak could be identified.
[c]Agrees with previously observed levels in ^{112}Cd but not observed in the $(n, n'\gamma)$ experiment [18].

the (d, p) and (d, t) transfers to ^{112}Cd. The differential cross section at $\theta = 15^\circ$ appears slightly raised in comparison with that of other nearby 0^+ states. It is noted that several of the $I^\pi = 2^+$ levels near 2.8 MeV are very weakly populated in the current work with $S_{\ell j} \sim 0.03$. If a doublet does exist, the lack of observation of the 0^+ level in the $(n, n'\gamma)$ experiment implies that it lies very close in energy such that the γ-ray decays were unresolved from those of the 2^+ state.

8. 2868 keV levels

A level consistent with spin 3 was observed at 2867.5 keV by Garrett *et al.* [18], which had previously been assigned as an $I^\pi = 3^+$ state in the $(\vec{d}, t)$ study [27]. This latter assignment is confirmed by the observation in the current work of a dominant $g_{\frac{7}{2}}$ transfer to a level at 2867.94(8) keV [49]. Evidence was also found for the presence of a 3^- state, which was weakly populated in the $(\vec{d}, p)$ reaction via an $f_{\frac{5}{2}}$ transfer, with $S_{\ell j} = 0.02$, thus supporting the conclusion by Garrett *et al.* [18] of a doublet of levels at 2868 keV.

9. 2899 keV level

A $J = 5$ level was previously observed at 2899 keV, and tentatively assigned as a 5^- state in the $(n, n'\gamma)$ study by Garrett *et al.* [18]. In the current work, a dominant $h_{\frac{11}{2}}$ transfer was observed [49] to a level at 2899.01(11) keV confirming the spin-parity assignment of 5^- to this level.

10. 2924 keV levels

A tentative assignment of $I^\pi = 5^-$ was previously made in a (d, d') reaction [51] for a level at 2922 keV. This level was reassigned by Garrett *et al.* [18] to $I^\pi = 4^-$. The current work confirms the latter assignment with the observation of a level at 2924.5(3) keV dominated by an $f_{\frac{7}{2}}$ transfer [49]. No evidence was found in the current work of a 0^+ state at 2924 keV observed in the $(\vec{d}, t)$ study [28]. The lack of observation of this latter level is consistent with the $(n, n'\gamma)$ study by Garrett *et al.* [18].

11. 2947 keV levels

A doublet of levels was proposed by Blasi *et al.* [28] at 2945 keV with $I^\pi = (2^+$ or $3^+)$ and $(3^+$ or $4^+)$. Drissi *et al.* [50] confirmed only the 2^+ assignment. The $(n, n'\gamma)$ study by Garrett *et al.* [18] found a doublet of levels with $I^\pi = 2^+$ at 2944.9 keV and $I^\pi = 3^+$ at 2947.8 keV. In the current work the 2^+ level was not observed. A level dominated by a $f_{\frac{7}{2}}$ transfer [49] was observed at 2946.98(8) keV, consistent with either $I^\pi = 3^-$ or $I^\pi = 4^-$.

12. 3002 keV level

Previous studies, most recently by Garrett *et al.* [18] have tentatively assigned a 3^+ level at 3002 keV [18]. The observation of a $g_{\frac{7}{2}}$ dominated transfer to a level at 3002.2(4) keV [49] in the current study confirms this assignment.

13. 3067 keV levels

A level at 3066 keV with has been assigned to have $I^\pi = 3^-$, along with a level at 3069 keV with $I^\pi = 4^+$ [48]. In the current study, a level was observed at 3067.10(10) keV, but the transfer is dominated by a $s_{\frac{1}{2}}$ component [49], consistent with $I^\pi = 0^+$. It is unclear why this level was not observed in the $(n, n'\gamma)$ study [18]. There is no evidence in the angular distributions of cross sections and analyzing powers from the current work of a transfer consistent with population of 3^- or a 4^+ levels, but these may be too weakly populated to be observed.

14. 3071 keV levels

A doublet of levels at 3069 keV was tentatively assigned with $I^\pi = (1^+$ or $2^+)$ and $(3^+$ or $4^+)$ [28]. In the current work, a $d_{\frac{3}{2}}$ dominated transfer was observed to a level at 3073.7(3) keV [49]. This observation is consistent with both $I^\pi = 1^+$ and 2^+. No contributions for transfer to a 3^+ or 4^+ level were evident from the angular distributions.

15. 3110 keV levels

In the current work, a doublet of levels was found near 3110 keV, with energies 3107.9(3) and 3111.6(3) keV dominated by $p_{\frac{3}{2}}$ and $d_{\frac{3}{2}}$ transfers, respectively [49]. Previously, a 2^+ level was assigned at 3108 keV, and the $(n, n'\gamma)$ study found evidence of a $J = 2, 3$ level at 3106 keV [18]. Garrett *et al.* [18] also observed a level at 3109.86(6) keV consistent with $I = 1$. The evidence suggests that the level observed in the current study at 3111.6(3) keV is $I^\pi = 1^+$, with the level at 3108 keV corresponding to the previously observed 3106 keV level, and could be assigned either as an $I^\pi = 1^-$ or $I^\pi = 2^-$ level; the lack of a ground state transition, however, favors the 2^- assignment.

16. 3130 keV levels

A doublet of levels was previously assigned at 3131 keV with spin-parities (5^- or 6^-) and 3^- [48]. The former was assigned unambiguously as a $I^\pi = 5^-$ state in the $(n, n'\gamma)$ study, while the later was not observed [18]. In the current work a transfer dominated by an $f_{\frac{7}{2}}$ component was observed at 3130.1(2) keV [49]. This is consistent with the existence of a 3^- state. No evidence was found for a 5^- contribution, but it may be too weakly populated for observation, nor was any evidence found for population of a 1^- state reported at 3133 keV [18]. It is thus unclear why it was not observed in the $(n, n'\gamma)$ reaction.

17. 3151.6 keV level

A new level was observed at 3151.6(3) keV, dominated by a $d_{\frac{3}{2}}$ transfer [49], consistent with $I^\pi = 1^+$ or 2^+. No candidate target impurity could be identified. Unlike some of the other suggested new levels, where γ-ray transitions to the ground state or first 2^+ state might be unresolved from neighboring transitions, the location of this level should have enabled easy identification of the decaying γ ray in the $(n, n'\gamma)$ study [18].

18. 3170 keV levels

A level was previously assigned as $I^\pi = 3^-$ with an energy of 3175(4) [48], but was not observed in the $(n, n'\gamma)$ study by Garrett *et al.* [18]. In the current work, a transfer was observed to a level at 3168.9(3) keV, dominated by an $f_{\frac{5}{2}}$ contribution [49], which is consistent with $I^\pi = 3^-$. There may be evidence from the angular distribution for population of a 2^+ level assigned at 3169.56(3) keV [18], but the spectroscopic factor for this contribution is small, with $S_{\ell j} \approx 0.007$.

19. 3194 keV level

An $I = 2$ level was proposed at 3190 keV and later confirmed to be 2^+, with a possible $2^+, 3^+$ level nearby at 3194 keV, by Garrett *et al.* [18]. The 2^+ assignment for one of these levels, favored to be the higher member of the doublet, was confirmed in the current work by the observation of a $d_{\frac{3}{2}}$ transfer to a level at 3194 keV [49].

20. 3203 keV level

An $I = 3$ level at 3203 keV was first observed in the $(n, n'\gamma)$ study [18], and tentatively assigned with positive parity. This assignment is confirmed in the current study by the observation of a $g_{\frac{7}{2}}$ dominated transfer [49] into a level at 3202.8(4) keV. Evidence was found of a $d_{\frac{5}{2}}$ component for this level in the current work [49], with $S_{\ell j} \approx 0.002$. Both contributions are consistent with an $I^\pi = 3^+$ assignment.

IV. INTERPRETATIONS

A. Two quasineutron configurations

The single-nucleon transfer reaction, when performed on an odd-A target that can be described as a one-quasiparticle state, populates the two-quasiparticle components in the final state wave functions. Strong population of a state observed in these reactions implies that the two-quasiparticle component, of the form $j_t \otimes j_{\rm tr}$ where j_t is the target single-particle configuration, and $j_{\rm tr}$ is the configuration of the transferred particle, is a dominant component of the wave function. Collective states may be populated through the two-quasiparticle content in their wave functions; these must, however, be one-phonon states (or the one-phonon components of wave functions). Strong populations of states can therefore be used to rule out multiphonon configurations. This was used to refute the 5^- member of the quadrupole-octupole-coupled (QOC) quintuplet in Ref. [32]. In the discussion below, the two-quasiparticle nature of the states will be discussed, combining the result of the present work with those of the ^{113}Cd$(\vec{d}, t)^{112}$Cd reaction [28].

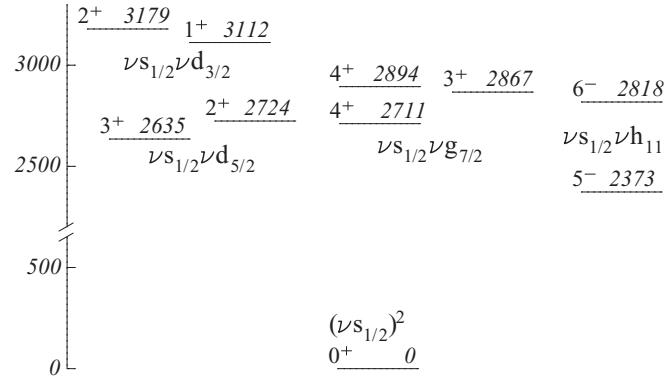

FIG. 5. States with dominant two-quasineutron configurations.

The target ground state of ^{111}Cd is assigned as the neutron $s_{\frac{1}{2}}$ configuration. The stripping reaction results in the transfer of a neutron into the ^{111}Cd target; it thus preferentially populates states above the Fermi surface. In the case of pure spherical shell model configurations, only a limited number of states would be populated: 0^+ from $(s_{\frac{1}{2}})^2$; 1^+, 2^+ from $s_{\frac{1}{2}}d_{\frac{3}{2}}$; 2^+, 3^+ from $s_{\frac{1}{2}}d_{\frac{5}{2}}$; 3^+, 4^+ from $s_{\frac{1}{2}}g_{\frac{7}{2}}$; 3^-, 4^- from $s_{\frac{1}{2}}f_{\frac{7}{2}}$; and 5^-, 6^- from $s_{\frac{1}{2}}h_{\frac{11}{2}}$. As can be seen from Table IV, far more states are populated than this limited number. In some cases, especially for the $d_{\frac{3}{2}}$ and $d_{\frac{5}{2}}$ orbitals, the strength is severely fragmented so that no state carries more than a small fraction. In others, as has already been outlined in Ref. [32] for the $s_{\frac{1}{2}}h_{\frac{11}{2}}$ configuration, definite assignments for the two-quasiparticle configurations can be made. Figure 5 displays the states assigned as having substantial two-quasineutron configurations. In the case of the $s_{\frac{1}{2}}g_{\frac{7}{2}}$ 4^+ state, there are two states close in energy that have nearly equal $g_{\frac{7}{2}}$ transfer strengths in both the (d, p) and (d, t) reactions.

1. The $(s_{\frac{1}{2}})^2$ configuration

The ground state was populated with the largest $\ell = 0$ strength observed in the present work. In the ^{113}Cd$(\vec{d}, t)^{112}$Cd study [28], the ground state was populated with strength of $S_{0,\frac{1}{2}} = 1.14$, implying that the neutron component of the ground state wave function is dominated by the $(s_{\frac{1}{2}})^2$ configuration. The 1224 and 1433 keV levels were weakly populated in the $(\vec{d}, p)$ reaction, and were not observed in the $(\vec{d}, t)$ study

[28]. Of the remaining 0^+ states, only the level at 2300 keV was populated with a non-negligible strength in both the $(\vec{d}, p)$ and $(\vec{d}, t)$ reactions.

2. The $s_{\frac{1}{2}} d_{\frac{3}{2}}$ configuration

The coupling of the $s_{\frac{1}{2}}$ and $d_{\frac{3}{2}}$ orbitals should yield two states, 1^+ and 2^+, that should be strongly populated in the single-neutron transfer reaction. A very strongly populated 1^+ state was observed at 3112 keV with $S_{2,\frac{3}{2}} = 0.83$, indicating that its dominant component is the $s_{\frac{1}{2}} d_{\frac{3}{2}}$ configuration. The 2^+ state with the strongest $d_{\frac{3}{2}}$ transfer population is in close proximity, at 3179 keV, with $S_{2,\frac{3}{2}} = 0.51$. It is seen that the $d_{\frac{3}{2}}$ transfer strength is highly fragmented in ^{112}Cd.

3. The $s_{\frac{1}{2}} d_{\frac{5}{2}}$ configuration

The coupling of the $s_{\frac{1}{2}}$ and $d_{\frac{5}{2}}$ orbitals yields states with $I^\pi = 2^+$ and 3^+. The levels populated with the greatest $d_{\frac{5}{2}}$ transfer strength are the 3^+ level at 2635 keV, with $S_{2,\frac{5}{2}} = 0.44$ in the (d, t) reaction [28] and $S_{2,\frac{5}{2}} = 0.2$ in the $(\vec{d}, p)$ reaction, and the 2^+ level at 2724 keV with $S_{2,\frac{5}{2}} = 0.4$ in the (d, t) reaction [28] and 0.22 in the (d, p) reaction. These levels have significant fractions of the $s_{\frac{1}{2}} d_{\frac{5}{2}}$ configuration in their wave functions, but it is unlikely to form an admixture greater than 50%. As with the $d_{\frac{3}{2}}$ strength, the $d_{\frac{5}{2}}$ strength is greatly fragmented amongst excited states in ^{112}Cd.

4. The $s_{\frac{1}{2}} g_{\frac{7}{2}}$ configuration

The levels with the greatest $g_{\frac{7}{2}}$ transfer strength are the 3^+ state at 2867 keV with $S_{4,\frac{7}{2}} = 0.55$ in the $(\vec{d}, p)$ reaction, and $S_{4,\frac{7}{2}} = 0.65$ in the $(\vec{d}, t)$ reaction [28]. Two 4^+ states share the greatest fraction of the $\ell = 4$ transfer strength; the states at 2711 and 2894 keV with $S_{4,\frac{7}{2}} = 0.51$ and 0.36, respectively, in the $(\vec{d}, p)$ reaction, and $S_{4,\frac{7}{2}} = 0.37$ and 0.45, respectively, in the $(\vec{d}, t)$ reaction. As with the $s_{\frac{1}{2}} d_{\frac{5}{2}}$ configuration, it is unlikely that the $s_{\frac{1}{2}} g_{\frac{7}{2}}$ configuration forms the dominant component of the 4^+ wave functions. These levels were also observed in an inelastic scattering experiment [52] with $B(E4\uparrow) = 3.6(4)$ and 4.7(5) W.u., and form part of the highly fragmented hexadecapole phonon state.

5. The $s_{\frac{1}{2}} h_{\frac{11}{2}}$ configuration

The $s_{\frac{1}{2}} h_{\frac{11}{2}}$ configuration was discussed in Ref. [32], where the 5^- member was assigned at 2373 keV and the 6^- member at 2818 keV. They were populated in the (d, p) reaction with $S_{5,\frac{11}{2}} = 2.7$ and 6.1, respectively, and in the (d, t) reaction with $S_{5,\frac{11}{2}} = 0.2$ and 0.6. These spectroscopic factors indicate that the $s_{\frac{1}{2}} h_{\frac{11}{2}}$ configuration is the dominant component of the wave function of these levels. The 5^- state at 2373 keV was also observed to be strongly populated in inelastic scattering experiments with $\beta_5 \approx 0.05$ [53], indicating a collective dotriacontapole component. The $\nu s_{\frac{1}{2}} h_{\frac{11}{2}}$ configuration, with $\Delta l = \Delta j = 5$, may be an important microscopic component of such a collective state.

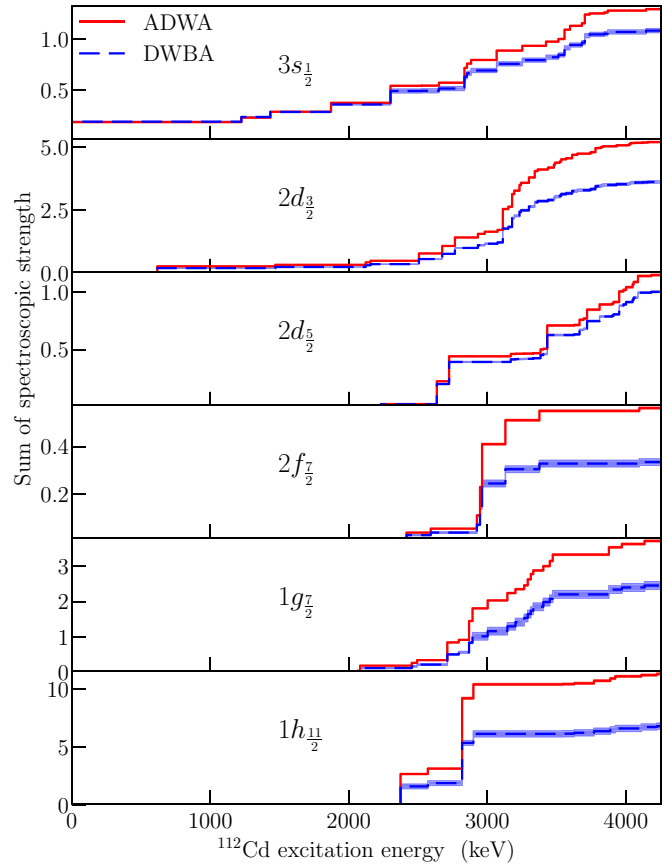

FIG. 6. Sums of strengths for each j-transfer value from the ^{111}Cd$(\vec{d}, p)^{112}$Cd as a function of the excitation energy.

B. Sum rules

The summed strength of a single neutron transfer with total transferred angular momentum j should equal the number of particles or holes occupying the j orbital in the target for pickup or stripping reactions respectively. Figure 6 shows the sum strength observed in the present work for each j transfer as a function of the excitation energy for strengths extracted using the ADWA and DWBA calculations. Summing the total strength for a j transfer from both the single-particle pickup and stripping reactions on a given target nucleus, the result should be

$$N_j^h + N_j^p = 2j + 1, \tag{12}$$

where N_j^h and N_j^p are the numbers of holes and particles in the j orbital of the target. The total sum of strength from a stripping reaction should equal the sum of valence holes in the ground state of the target nucleus. The ^{111}Cd$(\vec{d}, t)^{110}$Cd pickup reaction studied by Blasi *et al.* [27] used a 22 MeV polarized deuteron beam, as in the present study, and states states up to 4.2 MeV were identified. They adopted an overall 30% uncertainty associated with their choice of optical potential in the DWBA analysis. Table V lists the sums of strengths observed in the present work.

The total $s_{\frac{1}{2}}$ strength from both the stripping and pickup reactions sums to about 2.3, which agrees well with the sum rule given the uncertainties in the measured spectroscopic

TABLE V. Sums of strengths for $\ell = 0$–5 transfers in the ^{111}Cd$(\vec{d}, p)^{112}$Cd reaction. Uncertainties are quoted in parentheses and do not include the contribution due to the reaction modeling or choice of optical model parameters.

ℓ_j	$3s_{\frac{1}{2}}$	$3p_{\frac{1}{2}}$	$3p_{\frac{3}{2}}$	$2d_{\frac{3}{2}}$	$2d_{\frac{5}{2}}$
DWBA	1.08(2)	0.0081(2)	0.143(4)	3.60(4)	1.00(5)
ADWA	1.29(4)	0.0079(2)	0.132(4)	5.19(2)	1.15(7)
ℓ_j	$2f_{\frac{5}{2}}$	$2f_{\frac{7}{2}}$	$1g_{\frac{7}{2}}$	$1h_{\frac{11}{2}}$	
DWBA	0.072(4)	0.335(13)	2.46(11)	6.8(3)	
ADWA	0.052(3)	0.562(4)	3.73(2)	11.3(2)	

strengths. The DWBA strength for the $d_{\frac{3}{2}}$ transfers also agrees well with the sum rule, whereas the ADWA strength for these states seems to overestimate by about 60%. The ADWA calculation agrees well with the sum rule for the $g_{\frac{7}{2}}$ and $h_{\frac{11}{2}}$ transfers, while the DWBA analysis suggests that ∼20% and ∼35%, respectively, of the strength is not observed. Both reaction models suggest that less than 50% of the $d_{\frac{5}{2}}$ strength is observed.

The sum rule analysis, summarized in Table VI, indicates that the strengths from $3s_{\frac{1}{2}}$, $2d_{\frac{3}{2}}$, and $1h_{\frac{11}{2}}$ levels are almost entirely accounted for by the transfer into states below 4.2 MeV. The strength of the $2d_{\frac{5}{2}}$ orbitals, however, may be fragmented above 4.2 MeV. However, some of the $d_{\frac{5}{2}}$ strength from the present $(\vec{d}, p)$ reaction might be mixed with 2^+ and 3^+ levels that are dominated by the transfer allocated to the $2d_{\frac{3}{2}}$ and $1g_{\frac{7}{2}}$ orbitals, respectively. In the former case, the distorted wave calculations did not reproduce the pure $d_{\frac{3}{2}}$ and $d_{\frac{5}{2}}$ states well enough to determine contributions from multiple j transfers. In the latter case, the angular distribution of cross sections should have indicated multiple ℓ transfers, but, if the $\ell = 2$ transfer strength was small compared with the $\ell = 4$ transfer, it might not have been observable.

The centroid energies for the single-particle states observed are 2.43 MeV for the $s_{\frac{1}{2}}$, 3.00 MeV for the $d_{\frac{3}{2}}$, and 2.80 MeV for the $h_{\frac{11}{2}}$. The centroid for the observed $d_{\frac{5}{2}}$ and $g_{\frac{7}{2}}$ strengths are 3.30 and 3.07 MeV, respectively, but, since there are significant unaccounted strengths, the true centroids are likely higher in energy. Insufficient strength was observed for other orbitals to allow for any meaningful conclusions on their energy centroids.

TABLE VI. Strengths from ^{111}Cd$(\vec{d}, p)^{112}$Cd and ^{111}Cd$(\vec{d}, t)^{110}$Cd [27], for single-particle states between the $N = 50$ and $N = 82$ shell closures.

State	Sum of strengths			$\sum$(strip+pickup)		$2j+1$
	ADWA	DWBA	^{111}Cd$(\vec{d}, t)$	ADWA	DWBA	
$3s_{\frac{1}{2}}$	1.3	1.1	1.1	2.4	2.2	2
$2d_{\frac{3}{2}}$	5.2	3.6	0.8	6.0	4.4	4
$2d_{\frac{5}{2}}$	1.1	1.0	1.6	2.7	2.6	6
$1g_{\frac{7}{2}}$	3.7	2.5	2.7	6.4	5.2	8
$1h_{\frac{11}{2}}$	11.3	6.8	0.5	11.8	7.1	12

V. CONCLUSIONS

Levels in ^{112}Cd were investigated with the ^{111}Cd$(\vec{d}, p)$ reaction with 22 MeV deuterons with a polarization of $P = 0.80(4)$. Cross sections and analyzing powers for 129 levels, of which 49 are newly observed, were determined. The experimental angular distributions were compared with both DWBA and ADWA calculations. The ADWA calculations give a better reproduction of the angular distributions of the cross sections for $\ell = 0$ transfer. For the $\ell \neq 0$ transfers, there are variations from state to state such that the ADWA and DWBA calculations are equally as good. Considering the analyzing powers, the DWBA generally provides a better description, but also with variations from state to state. The levels observed are interpreted in terms of the two quasiparticle states with orbitals coupled to the $s_{\frac{1}{2}}$ neutron from the ^{111}Cd target. As reported previously [32], based on the current data an important reassignment of the 5^- member of the quadrupole-octupole-coupled quintuplet to the $s_{\frac{1}{2}}h_{\frac{11}{2}}$ configuration was made, questioning the appropriateness of the heterogeneous two-phonon assignments. Combining the results from a previous ^{111}Cd$(\vec{d}, t)$ study, the sum rules are approximately obeyed for the $s_{\frac{1}{2}}$, $d_{\frac{3}{2}}$, and $h_{\frac{11}{2}}$ orbitals, with less than 50% of the $d_{\frac{5}{2}}$ and 65–80% of the $g_{\frac{7}{2}}$ sum rule observed.

ACKNOWLEDGMENT

This work was supported in part by the Natural Sciences and Engineering Research Council (Canada).

[1] J. Kern, P. E. Garrett, J. Jolie, and H. Lehmann, Nucl. Phys. A **593**, 21 (1995).
[2] P. E. Garrett, K. L. Green, and J. L. Wood, Phys. Rev. C **78**, 044307 (2008).
[3] P. E. Garrett and J. L. Wood, J. Phys. G **37**, 064028 (2010); **37**, 069701(E) (2010).
[4] P. E. Garrett, J. Bangay, A. Diaz Varela, G. C. Ball, D. S. Cross, G. A. Demand, P. Finlay, A. B. Garnsworthy, K. L. Green, G. Hackman, C. D. Hannant, B. Jigmeddorj, J. Jolie, W. D. Kulp, K. G. Leach, J. N. Orce, A. A. Phillips, A. J. Radich, E. T. Rand, M. A. Schumaker, C. E. Svensson, C. Sumithrarachchi, S. Triambak, N. Warr, J. Wong, J. L. Wood, and S. W. Yates, Phys. Rev. C **86**, 044304 (2012).
[5] A. E. Stuchbery, S. K. Chamoli, and T. Kibédi, Phys. Rev. C **93**, 031302(R) (2016).
[6] P. E. Garrett, J. L. Wood, and S. W. Yates, Phys. Scr. **93**, 063001 (2018).
[7] J. Kern, A. Bruder, S. Drissi, V. A. Ionescu, and D. Kusnezov, Nucl. Phys. A **512**, 1 (1990).
[8] J. Kumpulainen, R. Julin, J. Kantele, A. Passoja, W. H. Trzaska, E. Verho, and J. Vaaramaki, Z. Phys. A **335**, 109 (1990).

[9] J. Kumpulainen, R. Julin, J. Kantele, A. Passoja, W. H. Trzaska, E. Verho, J. Vaaramaki, D. Cutoiu, and M. Ivascu, Phys. Rev. C **45**, 640 (1992).

[10] M. Délèze, S. Drissi, J. Kern, P. A. Tercier, J.-P. Vorlet, J. Rikovska, T. Otsuka, S. Judge, and A. Williams, Nucl. Phys. A **551**, 269 (1993).

[11] M. Délèze, S. Drissi, J. Jolie, J. Kern, and J.-P. Vorlet, Nucl. Phys. A **554**, 1 (1993).

[12] S. Juutinen, R. Julin, P. Ahonen, C. Fahlander, J. Hattula, J. Kumpulainen, A. Lampinen, T. Lonnroth, D. Muller, J. Nyberg, A. Pakkanen, M. Piiparinen, I. Thorslund, S. Tormanen, and A. Virtanen, Z. Phys. A **336**, 475 (1990).

[13] S. Juutinen, R. Julin, M. Piiparinen, P. Ahonen, B. Cederwall, C. Fahlander, A. Lampinen, T. Lonnroth, A. Maj, S. Mitarai, D. Muller, J. Nyberg, P. Simecek, M. Sugawara, I. Thorslund, S. Tormanen, A. Virtanen, and R. Wyss, Nucl. Phys. A **573**, 306 (1994).

[14] A. Gade, J. Jolie, and P. von Brentano, Phys. Rev. C **65**, 041305(R) (2002).

[15] A. Gade, A. Fitzler, C. Fransen, J. Jolie, S. Kasemann, H. Klein, A. Linnemann, V. Werner, and P. von Brentano, Phys. Rev. C **66**, 034311 (2002).

[16] F. Corminboeuf, T. B. Brown, L. Genilloud, C. D. Hannant, J. Jolie, J. Kern, N. Warr, and S. W. Yates, Phys. Rev. Lett. **84**, 4060 (2000).

[17] F. Corminboeuf, T. B. Brown, L. Genilloud, C. D. Hannant, J. Jolie, J. Kern, N. Warr, and S. W. Yates, Phys. Rev. C **63**, 014305 (2000).

[18] P. E. Garrett, H. Lehmann, J. Jolie, C. A. McGrath, M. Yeh, W. Younes, and S. W. Yates, Phys. Rev. C **64**, 024316 (2001).

[19] P. E. Garrett, K. L. Green, H. Lehmann, J. Jolie, C. A. McGrath, M. Yeh, and S. W. Yates, Phys. Rev. C **75**, 054310 (2007).

[20] D. Bandyopadhyay, S. R. Lesher, C. Fransen, N. Boukharouba, P. E. Garrett, K. L. Green, M. T. McEllistrem, and S. W. Yates, Phys. Rev. C **76**, 054308 (2007).

[21] M. Kadi, N. Warr, P. E. Garrett, J. Jolie, and S. W. Yates, Phys. Rev. C **68**, 031306(R) (2003).

[22] K. L. Green, P. E. Garrett, R. A. E. Austin, G. C. Ball, D. S. Bandyopadhyay, S. Colosimo, D. Cross, G. A. Demand, G. F. Grinyer, G. Hackman, W. D. Kulp, K. G. Leach, A. C. Morton, C. J. Pearson, A. A. Phillips, M. A. Schumaker, C. E. Svensson, J. Wong, J. L. Wood, and S. W. Yates, Phys. Rev. C **80**, 032502 (2009).

[23] A. Diaz Varela, P. E. Garrett, G. C. Ball, J. C. Bangay, D. S. Cross, G. A. Demand, P. Finlay, A. B. Garnsworthy, K. L. Green, G. Hackman, W. D. Kulp, K. G. Leach, J. N. Orce, A. A. Phillips, E. T. Rand, C. E. Svensson, C. Sumithrarachchi, S. Triambak, J. Wong, J. L. Wood, and S. W. Yates, Eur. Phys. J. Web Conf. **66**, 02029 (2014).

[24] B. Jigmeddorj, P. E. Garrett, A. Diaz Varela, G. C. Ball, J. C. Bangay, D. S. Cross, G. A. Demand, A. B. Garnsworthy, K. L. Green, G. Hackman, W. D. Kulp, K. G. Leach, J. N. Orce, E. T. Rand, C. Sumithrarachchi, C. E. Svensson, S. Triambak, J. Wong, J. L. Wood, and S. W. Yates, Eur. Phys. J. A **52**, 36 (2016).

[25] Y. Wang, P. Dendooven, J. Huikari, A. Jokinen, V. S. Kolhinen, G. Lhersonneau, A. Nieminen, S. Nummela, H. Penttila, K. Perajarvi, S. Rinta-Antila, J. Szerypo, J. C. Wang, and J. Aysto, Phys. Rev. C **64**, 054315 (2001).

[26] J. C. Batchelder, J. L. Wood, P. E. Garrett, K. L. Green, K. P. Rykaczewski, J.-C. Bilheux, C. R. Bingham, H. K. Carter, D. Fong, R. Grzywacz, J. H. Hamilton, D. J. Hartley, J. K. Hwang, W. Krolas, W. D. Kulp, Y. Larochelle, A. Piechaczek, A. V. Ramayya, E. H. Spejewski, D. W. Stracener, M. N. Tantawy, J. A. Winger, and E. F. Zganjar, Phys. Rev. C **80**, 054318 (2009).

[27] N. Blasi, S. Micheletti, M. Pignanelli, R. de Leo, R. Hertenberger, M. Bisemberger, D. Hofer, H. Kader, P. Schiemenz, and G. Graw, Nucl. Phys. A **536**, 1 (1992).

[28] N. Blasi, S. Micheletti, M. Pignanelli, R. de Leo, R. Hertenberger, F. J. Eckle, H. Kader, P. Schiemenz, and G. Graw, Nucl. Phys. A **511**, 251 (1990).

[29] P. D. Barnes, J. R. Comfort, and C. K. Bockelman, Phys. Rev. **155**, 1319 (1967).

[30] J. R. Comfort, C. K. Bockelman, and P. D. Barnes, Phys. Rev. **157**, 1065 (1967).

[31] Norman K. Glendenning, *Direct Nuclear Reactions* (Academic, New York, 1983).

[32] D. S. Jamieson, P. E. Garrett, V. Bildstein, G. A. Demand, P. Finlay, K. L. Green, K. G. Leach, A. A. Phillips, C. S. Sumithrarachchi, C. E. Svensson, S. Triambak, G. C. Ball, T. Faestermann, R. Hertenberger, and H.-F. Wirth, Phys. Rev. C **90**, 054312 (2014).

[33] P. E. Garrett, H. Lehmann, J. Jolie, C. A. McGrath, Minfang Yeh, and S. W. Yates, Phys. Rev. C **59**, 2455 (1999).

[34] G. Dollinger and T. Faestermann, Nucl. Phys. News **28**, 5 (2018).

[35] R. Hertenberger, A. Metz, Y. Eisermann, K. El Abiary, A. Ludewig, C. Pertl, S. Treib, H.-F. Wirth, P. Schiemenz, and G. Graw, Nucl. Instrum. Methods Phys. Res. A **536**, 266 (2005).

[36] H.-F. Wirth, H. Angerer, T. von Egidy, Y. Eisermann, G. Graw, and R. Hertenberger, Maier-Leibnitz Laboratorium Jahresbericht 2000 (unpublished), p. 71.

[37] I. J. Thompson, Comput. Phys. Rep. **7**, 167 (1988).

[38] W. W. Daehnick, J. D. Childs, and Z. Vrcelj, Phys. Rev. C **21**, 2253 (1980).

[39] J. Bojowald, H. Machner, H. Nann, W. Oelert, M. Rogge, and P. Turek, Phys. Rev. C **38**, 1153 (1988).

[40] H. An and C. Cai, Phys. Rev. C **73**, 054605 (2006).

[41] Y. Han, Y. Shi, and Q. Shen, Phys. Rev. C **74**, 044615 (2006).

[42] F. D. Becchetti and G. W. Greenlees, Phys. Rev. **182**, 1190 (1969).

[43] J. J. H. Menet, E. E. Gross, J. J. Malanify, and A. Zucker, Phys. Rev. C **4**, 1114 (1971).

[44] R. L. Varner, W. J. Thompson, T. L. McAbee, E. J. Ludwig, and T. B. Clegg, Phys. Rep. **201**, 57 (1991).

[45] A. J. Koning and J. P. Delaroche, Nucl. Phys. A **713**, 231 (2003).

[46] R. Petit, B. W. van der Pluym, P. J. van Hall, S. S. Klein, W. H. L. Moonen, G. J. Nijgh, C. W. A. M. van Overveld, and O. J. Poppema, J. Phys. G **20**, 1955 (1994).

[47] *Nuclear Reactions for Astrophysics: Principles, Calculation and Applications of Low-Energy Reactions*, edited by I. J. Thompson and F. M. Nunes (Cambridge University Press, Cambridge, UK, 2009).

[48] S. Lalkovski and F. G. Kondev, Nucl. Data Sheets **124**, 157 (2015).

[49] See Supplemental Material at http://link.aps.org/supplemental/10.1103/PhysRevC.98.044309 for the angular distributions and analyzing powers for the states above 2.7 MeV in excitation energy observed in the reaction.

[50] S. Drissi, P. A. Tercier, H. G. Börner, M. Délèze, F. Hoyler, S. Judge, J. Kern, S. J. Mannanal, G. Mouze, K. Schreckenbach,

J-.P. Vorlet, N. Warr, A. Williams, and C. Ythier, Nucl. Phys. A **614**, 137 (1997).

[51] R. Hertenberger, G. Eckle, F. J. Eckle, G. Graw, D. Hofer, H. Kader, P. Schiemenz, Gh. Cata-Danil, C. Hategan, N. Fujiwara, K. Hosono, M. Kondo, M. Matsuoka, T. Noro, T. Saito, S. Kato, S. Matsuki, N. Blasi, S. Micheletti, and R. de Leo, Nucl. Phys. A **574**, 414 (1994).

[52] M. Pignanelli, N. Blasi, S. Micheletti, R. de Leo, L. LaGamba, R. Perrino, J. A. Bordewijk, M. A. Hofstee, J. M. Schippers, S. Y. van der Werf, J. Wesseling, and M. N. Harakeh, Nucl. Phys. A **540**, 27 (1992).

[53] M. Pignanelli, N. Blasi, S. Micheletti, R. de Leo, M. A. Hofstee, J. M. Schippers, S. Y. van der Werf, and M. N. Harakeh, Nucl. Phys. A **519**, 567 (1990).